

# TRANSOPTR Implementation of the HEBT Beamlines

Olivier Shelbaya

TRIUMF

**Abstract:** Under the TRIUMF High-Level Applications (HLA) framework, the linear envelope optics code TRANSOPTR has been extended to include the ISAC High Energy Beam Transport (HEBT) section. On-axis electric field maps for the HEBT 11 and 35MHz bunchers, computed with *Opera-2D* for TRANSOPTR use are presented. The implementation of the HEBT lines in TRANSOPTR and a benchmark comparison with the code *trace3D*, used up to this point to perform the envelope optics computations used to produce HEBT tunes, is shown and discussed.

## Contents

<b>1</b>	<b>Introduction</b>	<b>2</b>
<b>2</b>	<b>High-Level Application Implementation</b>	<b>4</b>
<b>3</b>	<b>HEBT Sequences and Source Material</b>	<b>4</b>
3.1	Sequence hebt_db0 . . . . .	4
3.2	Sequence hebt_db9 . . . . .	7
3.3	Sequence hebt_db12 . . . . .	8
3.4	Sequence hebt_db16 . . . . .	11
3.5	Sequence hebt2_db0 . . . . .	13
3.6	Sequence hebt3_db0 . . . . .	14
<b>4</b>	<b>HEBT RF Cavities</b>	<b>16</b>
4.1	Opera2D RF Cavity Simulations . . . . .	17
<b>5</b>	<b>Trace-3D Simulations</b>	<b>22</b>
5.1	Trace-3D Element Setpoints . . . . .	31
<b>6</b>	<b>TRANSOPTR Implementation of the HEBT Beamlines</b>	<b>33</b>
<b>7</b>	<b>Conclusion</b>	<b>38</b>

## 1 Introduction

This note relates the extension of TRANSOPTR to the ISAC High-Energy Beam Transport (HEBT) beamlines, which define the network of beam delivery paths for the ISAC-I high energy experimental facility [1]. The present document is written in an analogous matter to, and should be considered a companion of, TRI-BN-19-02 [2] which covers the implementation of the MEBT beamline. The addition of HEBT to TRANSOPTR is part of an ongoing effort to allow for beam envelope simulations spanning the entirety of the ISAC facility, enabling end-to-end simulations of the ISAC accelerators and thereby permitting more efficient tuning and tune analysis, in addition to providing the requisite tools to physicists and operators to enable a planned reduction in tuning overhead.

HEBT is composed of a primary linear transport beamline, from which there are 4 branch-off points, in which dipole magnets allow transverse beam deflection into further transport beamlines, as shown in Figure 1. Heavy ion beams are injected into the main HEBT line after traversing the ISAC-I accelerator, which allows for a variable output energy of  $0.153\text{MeV/u} \leq E \leq 1.53\text{MeV/u}$  with  $2 \leq A/q \leq 7$ . A stripping foil in the first segment of the HEBT section, immediately following the DTL, allows for higher charge state selection, for the dual purposes of beam contaminant filtering and matching into the ISAC-II superconducting linac. Sequentially, the branch-off points for the HEBT section consist of:

- An S-Bend transfer section to ISAC-II (DSB),
- $90^\circ$  beam analyzing magnet (Prague),
- transport section to the DRAGON experiment (HEBT2),
- transport section to the TUDA-I experiment (HEBT3), and
- $0^\circ$  general purpose experimental station at the end of the main HEBT line

It is noted that the present implementation is defined up to the hand-off interface defining the boundaries between ISAC delivery and the experimental stations located beyond. As such, the beam transport sections belonging to the DRAGON and TUDA experiments are not explicitly covered in the present work.

The HEBT section contains two RF bunching cavities, located upstream of the HEBT2 branch-off point. These bunchers allow for time or energy focusing of beams at any of the ISAC-I high energy experiments serviced by the HEBT line.

This note will discuss the implementation of the HEBT transport optics and RF to TRANSOPTR in addition to a benchmark comparison to the envelope code `Trace-3D`, which was utilized up to this point for the computation of high energy tunes at ISAC. As was the case for TRI-BN-19-02 for the MEBT implementation, the comparison made herein is not intended as a test or commentary on either model's performance, but rather as a demonstration of the ability of the present TRANSOPTR implementation to reproduce and ultimately supplant the previous model for use in the computation and analysis of ISAC high energy tunes.

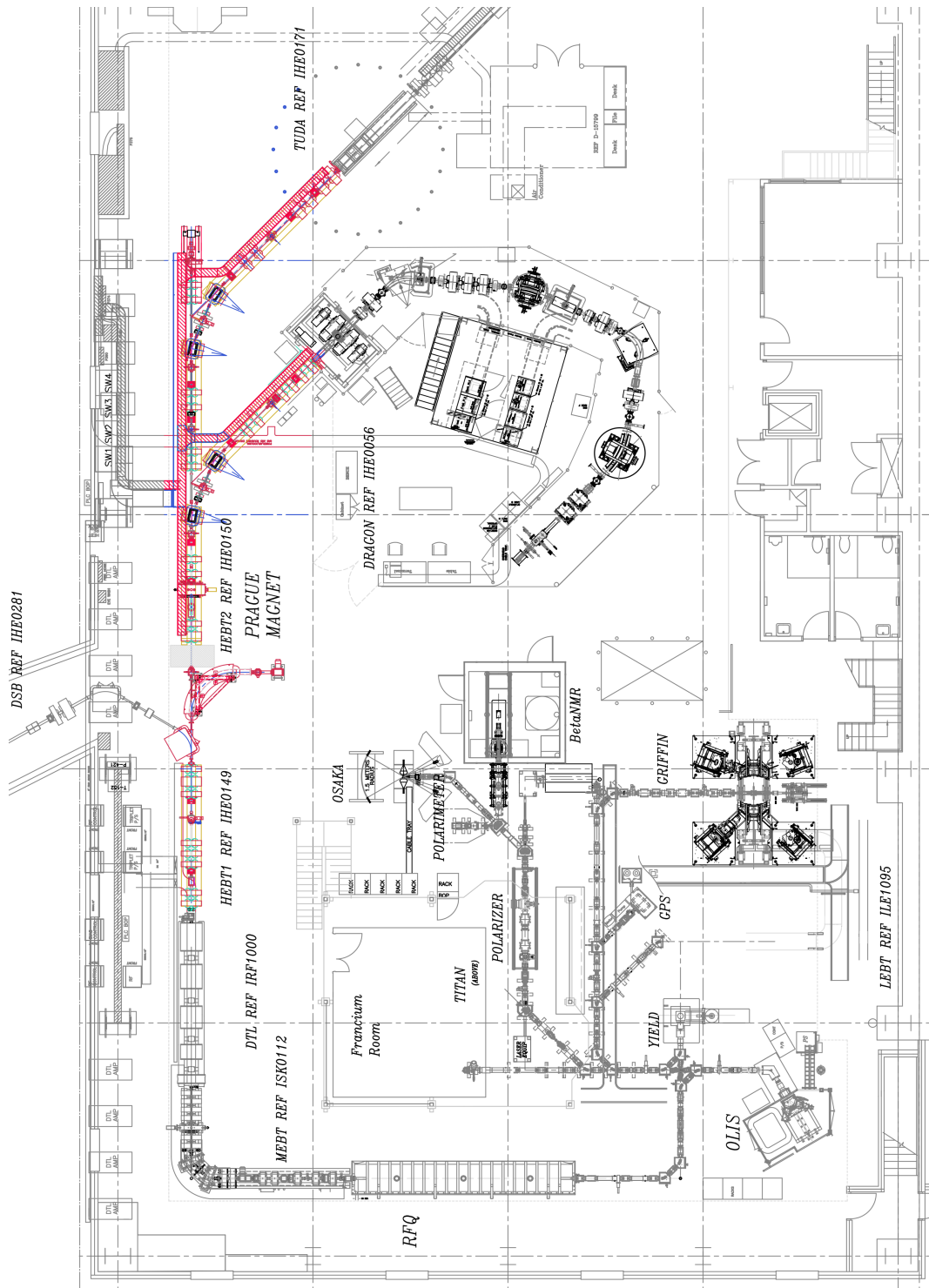


Figure 1: Overview of ISAC-I, with HEBT section highlighted in red.

## 2 High-Level Application Implementation

Under the TRIUMF High-Level Applications (HLA) framework [3], the traditional TRANSOPTR element sequence stack `sy.f` is automatically generated through a python wrapper routine, which reads in the requisite sequence of elements from a central database. This database, known as the `/acc` database, formatted in `xm1`, contains a sequential ordering of all transport, diagnostic and accelerating elements present along a given beamline segment. Within the database, groups of elements are broken down into sequences, which consist of the smallest possible number of sequential elements which define a unique path.

While the sequence `xm1` files contain the locations of all elements present in the beamline, including steering elements, beam diagnostics and aperture constrictions, for the purposes of the present note, these will be omitted from discussion, in favor of beamline optical elements such as quadrupoles and RF cavities. The rationale for doing so is that both diagnostics and steerers are not used in TRANSOPTR, which assumes an on-axis beam at all times and locations along the beampath. This is not to say that diagnostic locations are unimportant. On the contrary, knowing their precise location is crucial to predict measured beam envelope behavior. However, given that they do not affect the envelope TRANSOPTR, in the present note their presence is implicitly acknowledged but not explicitly discussed. Consequently, the focus will be placed on ion-optical elements such as quadrupoles, bending magnets and RF cavities.

## 3 HEBT Sequences and Source Material

All dimensions for the layout of the HEBT beamline were obtained from the TRIUMF Design Office. The present section details each sequence which was implemented for ISAC-I HEBT, along with the associated drawings from which element positions were measured. While the `/acc` database contains definitions of all elements represented in the design drawings, including diagnostics and vacuum elements, such as isolation valves, the sequences as presented herein will only list optical beamline elements, such as quadrupoles, magnetic dipoles and RF cavities. Further note that x and y steerers are also present in the database, but presently have no effect in TRANSOPTR, which assumes zero-value centroids for the beam distribution along the optical path.

The position S along the optical path for all sequences is referenced to the start of sequence marker, with the sequence ending at the end of sequence marker. Each sequence's ending point is made to precisely overlap with the beginning of the following one. In cases where the sequence measurements had to be extracted from more than one design drawing, this will be indicated in the sequence table. All sequence element locations are referenced to the design drawing shown immediately above to the element in question, where the drawing number, a link to the figure and the start and end (x,y) coordinates used for measurements are specified.

### 3.1 Sequence `hebt_db0`

The first sequence in HEBT begins at diagnostic box 0, immediately following DTL Tank-5 output and is defined up to the first DSB dipole magnet, at which point beam may continue

into HEBT or be deflected into DSB. Since sequences in the /acc database define unique nonoverlapping beam paths, the sequence `hebt_db0` is ended at the device immediately prior to the first DSB dipole. HEBT beams span an mass to charge ratio from  $2 \leq A/q \leq 7$ , the limiting factor being the bending power of the MEBT 90° dipoles, whose power supplies reach their output current limit just beyond  $A/q = 7$ .

sequence <code>hebt_db0</code>			
Start IHE0281D.dwg (x,y)		End IHE0281D.dwg (x,y)	
(1403.8054mm,11955.7177mm)		(1403.5516mm,6007.5647mm)	
Design Drawing		Figure 2	
Element Name	Element Type	Position S[mm]	Length L[mm]
start sequence	marker	0.000	0.000
HEBT:Q1	MQuad	714.600	180.000
HEBT:Q2	MQuad	1084.604	180.000
HEBT:Q3	MQuad	2109.600	180.000
HEBT:Q5	MQuad	2849.600	180.000
HEBT:STRP5	marker	3629.597	0.000
HEBT:Q6	MQuad	4619.600	180.000
HEBT:Q7	MQuad	5072.100	325.000
HEBT:Q8	MQuad	5524.600	180.000
end sequence	marker	5948.153	0.000

Table 1: Sequence `hebt_db0`, showing source design drawing (`.dwg` file) with reference start and end coordinates from which elements and their positions along the optical axis, S in millimeters were extracted. Note: design drawing `IHE0281D.dwg` uses millimeters as reference units, unlike many of the other ISAC-I drawings. The `TRANSOPTR` element (subroutine) type, in addition to the element length are also displayed. All element positions are referenced to the drawing listed above their respective location in the table. Note: HEBT:Q4 is absent from the database, as the quadrupole, while present on the beamline, is inoperative. Tunes through HEBT therefore use HEBT:Q3 and Q5 to compensate.

The location of the HEBT stripping foil is noted in Table 1 as HEBT:STRP5. The present `TRANSOPTR` implementation only allows for a single charge state through this section. A planned addition to `TRANSOPTR` will allow for a discrete charge state increase, with accompanying emittance growth. It is noted that without such a subroutine, charge state increase can still be simulated by breaking the sequence `hebt_db0` into two sub-sequences, before and after the stripping foil. Then, the discrete charge state increase and emittance growth fed into the following sub-sequence.

It is noted that the quadrupole HEBT:Q4 is omitted from the sequence as the device, while physically present around the beamline, is inoperative. Due to the complexity involved in its removal, it was chosen to simply leave it in place unpowered and use the quadrupoles HEBT:Q3 and Q5 in an alternate setting to compensate for the loss of Q4's effect upon the beam. As there are currently no plans to put Q4 back into service, for the present purposes it has been omitted from the database.

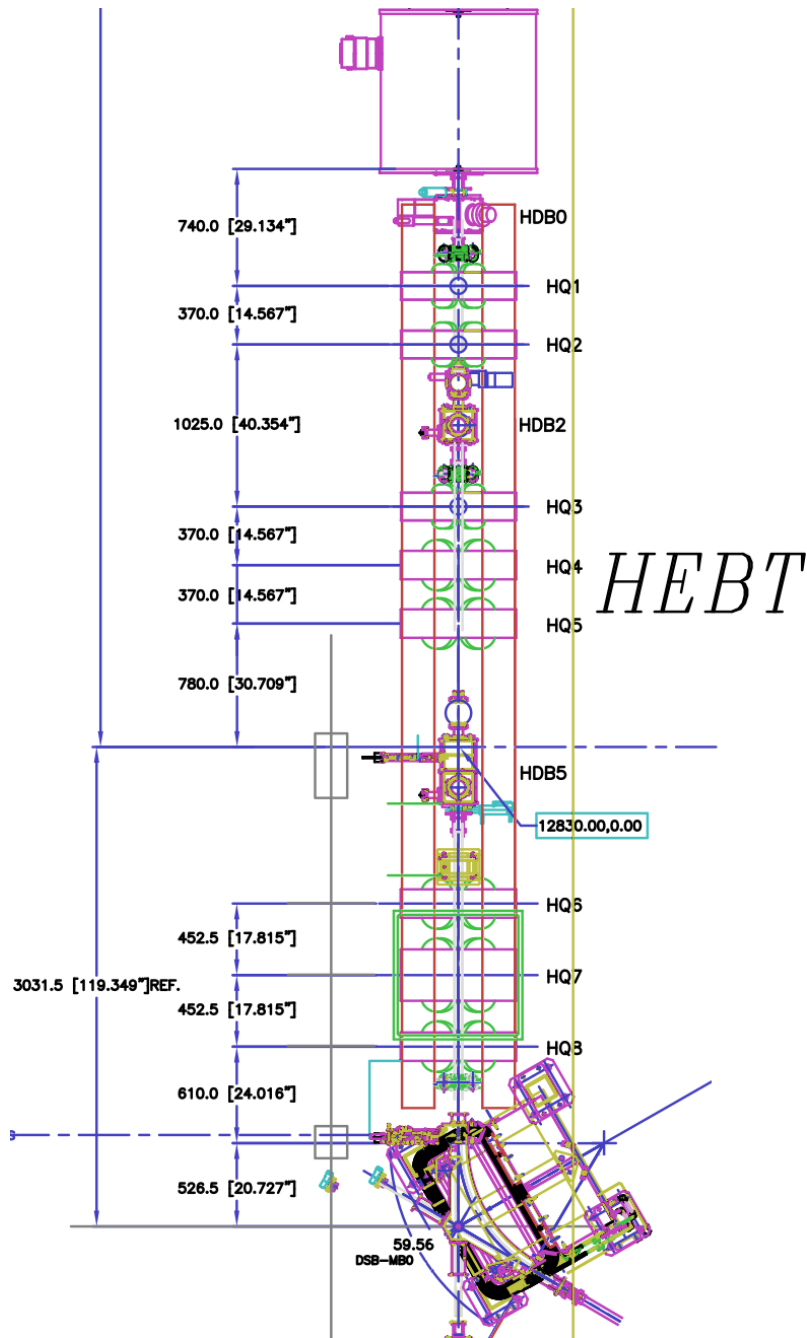


Figure 2: Design drawing IHE0281D.dwg, showing an overview of sequence `hebt_db0`, spanning HEBT:Q1 to HEBT:Q8. DTL Tank5 is visible at the very top, with the beam propagation direction running from top to bottom. Device HEBT:Q4 is present, however inoperative at the moment, and as such is excluded from the database. The first DSB dipole, MB0 (excluded from `hebt_db0`, is visible at the bottom of the figure.

### 3.2 Sequence hebt\_db9

Accelerated beam transport to either of the ISAC-I high energy experiment stations follows hebt\_db0 into the sequence hebt\_db9. The latter sequence contains quadrupoles HEBT:Q9 to HEBT:Q12, and includes both HEBT RF bunchers, enabling supplemental longitudinal beam focussing to meet experimental needs. The optical elements in the sequence are shown in Table 2. It is noted that the initial drift, carrying beam from HEBT:Q8 to HEBT:Q9 consists of a  $\sim 4.3\text{m}$  drift which traverses both DSB:MB0 and the Prague magnet (HEBT1:MB0).

During normal ISAC-I high energy delivery, both devices are turned off allowing unimpeded passage for the beam bunches. The sequence, measured from both IHE0281D.dwg and IHE0134D.dwg, is shown in Figure 3. It is noted that the initial drift leading up to Q9 is measured on IHE0281D.dwg up to the centerpoint of HEBT:Q9, at which point the sequence references are taken from IHE0134D.dwg, with HEBT:Q9 being a common element to both drawings. The sequence ends on IHE0281D.dwg at the point specified in Table 2, which coincides with the dipole magnet HEBT2:MB0. When the former is powered, beam is deflected laterally into the HEBT2 beamline for delivery to the DRAGON experiment. In particular, the sequence hebt\_db9 ends at the point in space defining the location of the branching off point of the curved reference trajectory through HEBT2:MB0, with respect to the straight trajectory through HEBT.

sequence hebt_db9			
Start IHE0281D.dwg (x,y)		End IHE0281D.dwg (x,y)	
(1403.805mm,6007.565mm)		(1403.805mm,1658.641mm)	
Design Drawing		Figure 2	
Element Name	Element Type	Position S[mm]	Length L[mm]
start sequence	marker	0.000	0.000
HEBT:Q9	MQuad	4348.924	325.000
Start IHE0134D.dwg (x,y)		End IHE0134D.dwg (x,y)	
(60.934",75.353")		(224.418",75.353)	
Design Drawing		Figure 3	
Element Name	Element Type	Position S[mm]	Length L[mm]
HEBT:Q10	MQuad	4802.390	180.000
HEBT:BUNCH11	linac	5796.267	703.834
HEBT:BUNCH35	linac	6468.173	390.423
HEBT:Q11	MQuad	7044.905	180.000
HEBT:Q12	MQuad	7574.902	180.000
end sequence	marker	8954.884	0.000

Table 2: Sequence hebt\_db9, showing source design drawings (.dwg files) with reference start and end coordinates from which elements and their positions along the optical axis, S in millimeters were extracted. Note: all HEBT design drawings use inches as reference units, however the /acc database by convention is defined in metric units. The TRANSOPT element (subroutine) type, in addition to the element length are also displayed. All element positions are referenced to the drawing listed above their respective location in the table.

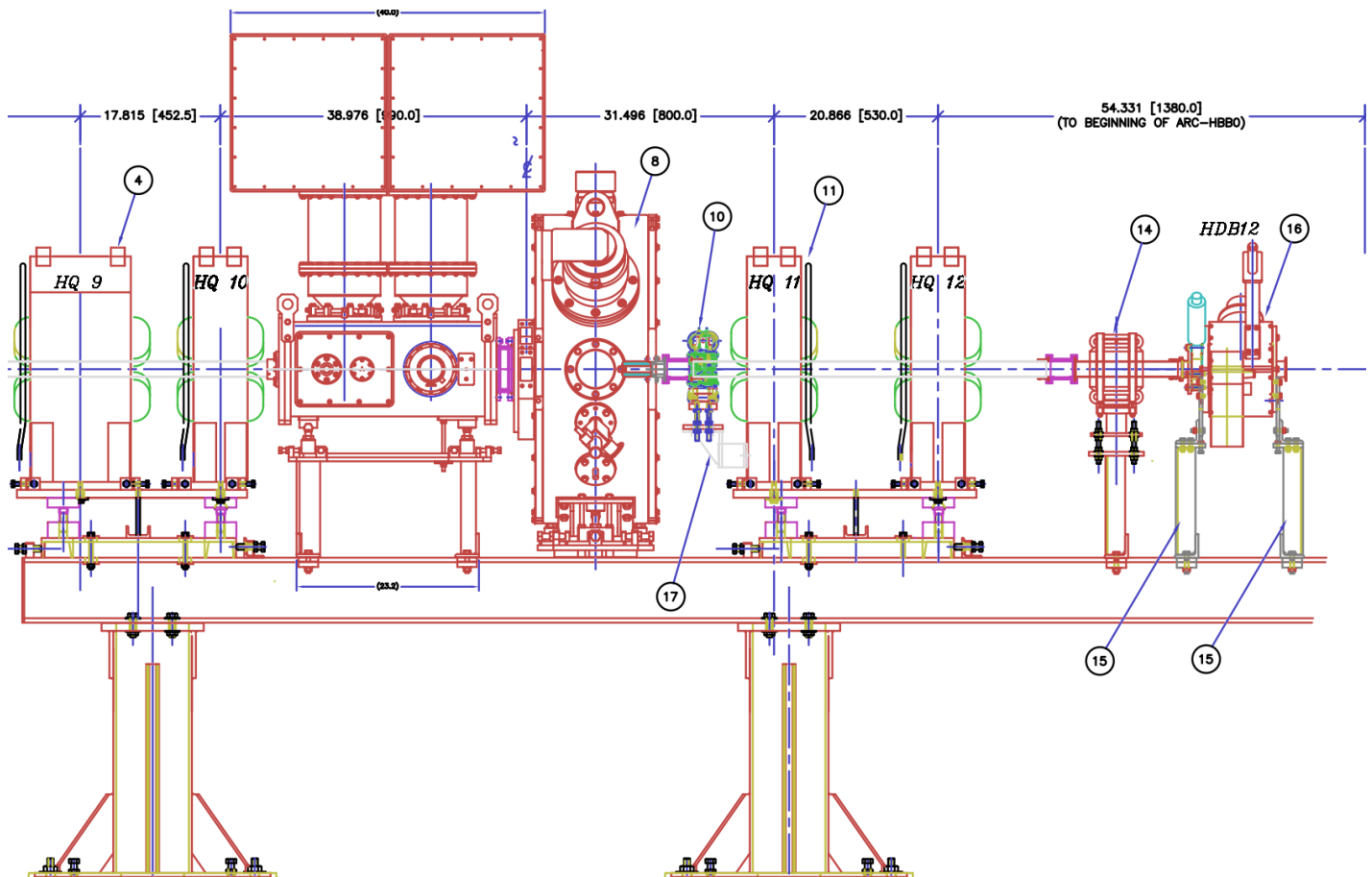


Figure 3: Design drawing IHE0134D.dwg, showing an overview of sequence `hebt_db9`, spanning HEBT:Q9 to HEBT:Q12. Note that the sequence starts with a drift referenced to drawing IHE0281D.dwg (Figure 2, at coordinates (1403.9468mm, 6007.5647mm), measured up to the central point of HEBT:Q9, after which the referencing of distances is switched to IHE0134D.dwg. Further note that both HEBT bunchers, the 11MHz low-beta and 35MHz high-beta are visible in the present figure, in sequence between HQ10 and HQ11. The beam propagation in the present figure runs from left to right.

### 3.3 Sequence `hebt_db12`

The next sequence in the HEBT section is `hebt_db12`, which consists of a straight beamline segment spanning HEBT2:MB0 to HEBT3:MB0, the latter being the horizontal deflecting dipole used for delivery to the TUDA-I experimental station. The sequence is defined using the design drawings listed in Table 3, including the sub sequences HEBT:Q12 to Q14 and HEBT:Q15 to Q16. The sequence ends at the device HEBT3:MB0, at the point in space where the curved reference trajectory through the dipole begins. Both drawings defining `hebt_db12` are shown in Figures 4 and 5.

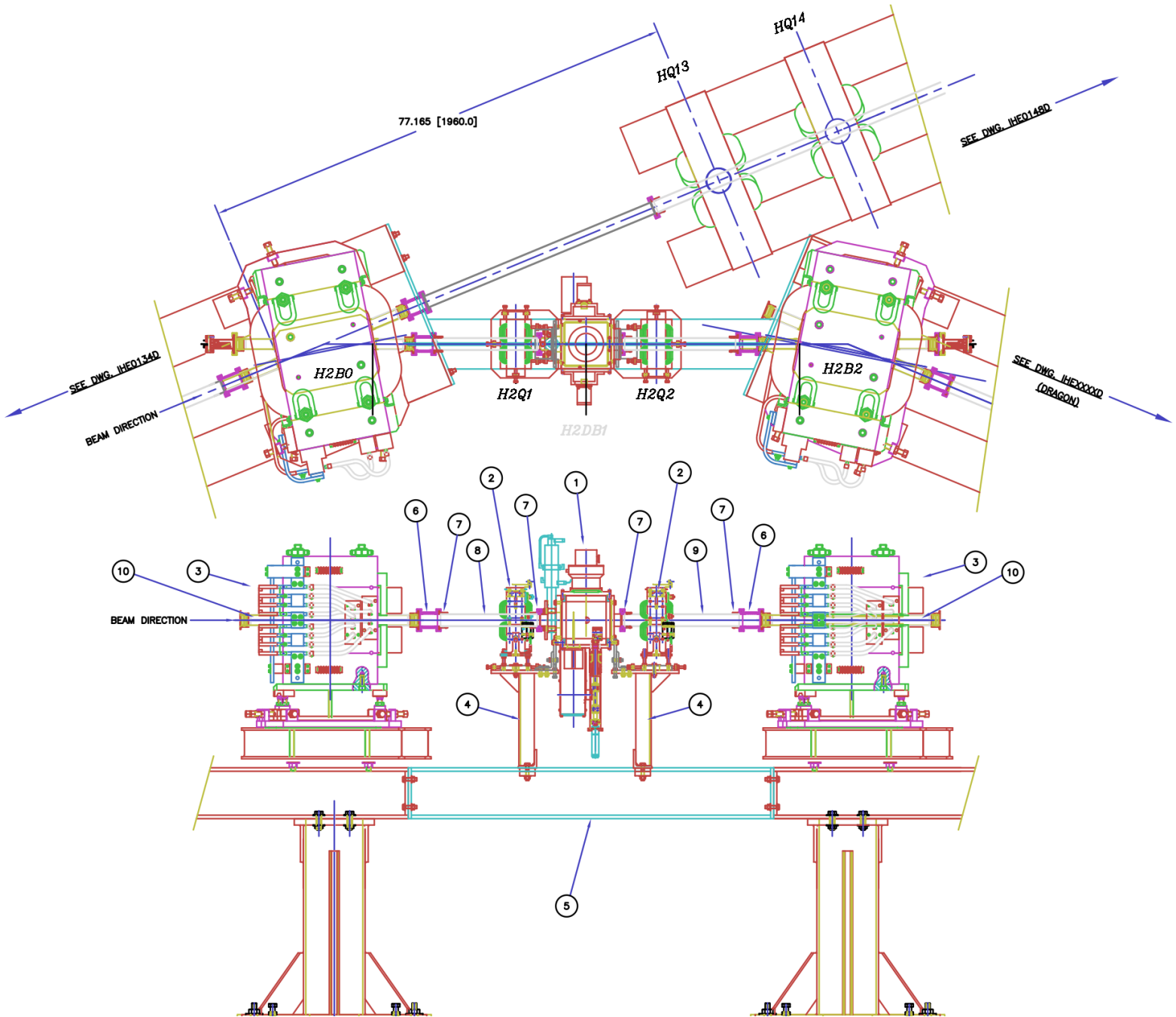


Figure 4: Design drawing IHE0120D.dwg, showing an overview of the first half of sequence hebt\_db12, spanning HEBT2:MB0 to HEBT:Q14. Note that the sequence assumes HEBT2:MB0 is off and does not deflect beam to DRAGON. The beam propagation in the present figure runs from left to right. Beyond HEBT:Q14, the reference for sequence hebt\_db12 switches to drawing IHE0148D.dwg, shown in Figure 5.

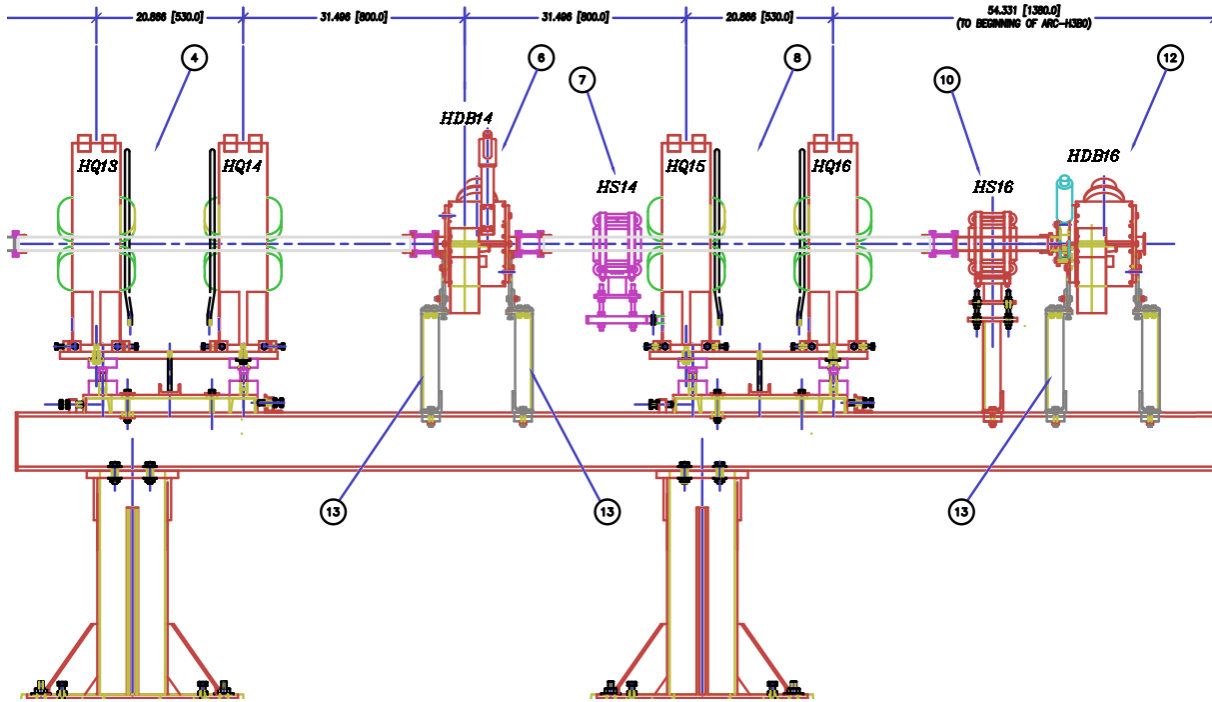


Figure 5: Design drawing IHE0148D.dwg, showing an overview of the second half of sequence hebt\_db12, spanning HEBT:Q14 to the end of sequence point, which is defined as the beginning of the curved reference trajectory through HEBT3:MB0. The beam propagation in the present figure runs from left to right. Prior to HEBT:Q14, the reference for sequence hebt\_db12 is defined in drawing IHE0120D.dwg, shown in Figure 4.

Quadrupole positions in hebt\_db12 are noted in Table 3.

sequence hebt_db12			
Start IHE0120D.dwg (x,y)		End IHE0120D.dwg (x,y)	
(50.382",115.593")		(140.963",152.108")	
Design Drawing		Figure 4	
Element Name	Element Type	Position S[mm]	Length L[mm]
HEBT2:MB0	marker	0.000	0.000
HEBT:Q13	MQuad	1960.271	180.000
Start IHE0148D.dwg (x,y)		End IHE0148D.dwg (x,y)	
(59.128",76.905")		(197.317",76.905")	
Design Drawing		Figure 5	
Element Name	Element Type	Position S[mm]	Length L[mm]
HEBT:Q14	MQuad	2490.275	180.000
HEBT:Q15	MQuad	4090.274	180.000
HEBT:Q16	MQuad	4620.273	180.000
end sequence	marker	6000.273	0.000

Table 3: Sequence hebt\_db12, showing source design drawings (.dwg files) with reference start and end coordinates from which elements and their positions along the optical axis, S in millimeters were extracted. Note: all HEBT design drawings use inches as reference units, however the /acc database by convention is defined in metric units. The TRANSOPTR element (subroutine) type, in addition to the element length are also displayed. All element positions are referenced to the drawing listed above their respective location in the table.

### 3.4 Sequence hebt\_db16

The final sequence defining the straight HEBT line is hebt\_db16, starting at the location of HEBT3:MB0 and defined up until the isolation valve HEBT:IV18. This sequence transports beam to the HEBT 0° experimental station, and assumes that the dipole HEBT3:MB0 is off. Inspection of Table 4 reveals that the sequence, in particular quadrupoles HEBT:Q17 and Q18 are referenced to the same drawing which contains the magnetic dipoles HEBT3:MB0 and MB1, shown in Figure 6. Seeing as the drawing excludes the isolation valve HEBT:IV18, the centerpoint of Q18 is the last point referenced to drawing IHE0129D.dwg after which the reference is switched to the overview drawing ISK0141D.dwg, for the distance from HEBT:Q18 to HEBT:IV18. The distances defining hebt\_db16 are shown in Table 4.

sequence hebt_db16			
Start IHE0129D.dwg (x,y)		End IHE0129D.dwg (x,y)	
(50.387",114.593")		(140.963",152.108")	
Design Drawing		Figure 6	
Element Name	Element Type	Position S[mm]	Length L[mm]
HEBT3:MB0	marker	0.000	0.000
HEBT:Q17	MQuad	1960.154	180.000
HEBT:Q18	MQuad	2490.157	180.000
Start ISK0141D.dwg (x,y)		End ISK0141D.dwg (x,y)	
(1154.132",3453.388")		(1197.886",3453.388")	
Design Drawing		Figure 7	
Element Name	Element Type	Position S[mm]	Length L[mm]
end sequence	marker	3601.509	0.000

Table 4: Sequence hebt\_db16, showing source design drawings (.dwg files) with reference start and end coordinates from which elements and their positions along the optical axis, S in millimeters were extracted. Note: all HEBT design drawings use inches as reference units, however the /acc database by convention is defined in metric units. The TRANSOPTR element (subroutine) type, in addition to the element length are also displayed. All element positions are referenced to the drawing listed above their respective location in the table.

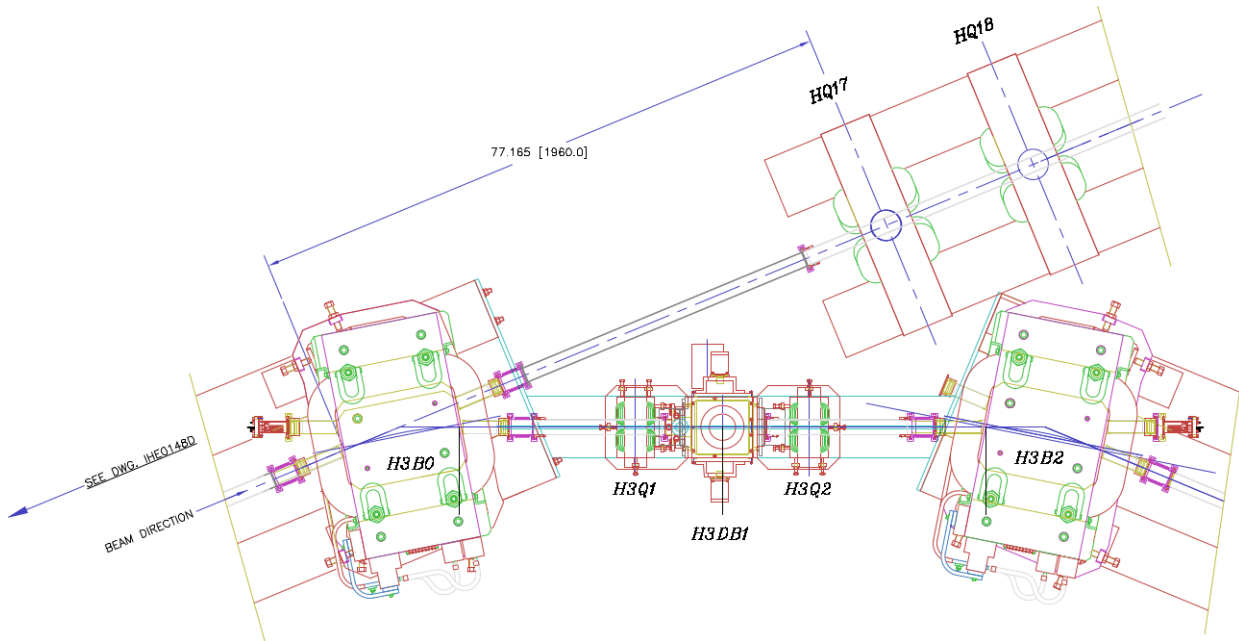


Figure 6: Design drawing ISK0129D.dwg, showing an overview of the first third of sequence hebt3\_db0, spanning HEBT3:MB0 to HEBT3:Q8. Note that the sequence hebt\_db16 assumes HEBT3:MB0 is off, with beam propagation following the 0° HEBT line into HEBT:Q17 and Q18, onward. The beam propagation in the present figure runs from left to right.

### 3.5 Sequence `hebt2_db0`

Beam delivery to DRAGON is enabled by both dipole magnets HEBT2:MB0 and HEBT2:MB1, which laterally deflect beam towards the HEBT2 line. As such, the sequence `hebt2_db0` is defined at the start of the curved reference trajectory through HEBT2:MB0, starting off where `hebt_db9` ends. The sub-sequences, design drawings and start/end points defining `hebt2_db0` are listed in Table 5. Beyond HEBT2:MB1, the remaining straight segment comprising the HEBT2 line is shown in Figure 7, with the overall layout of the sequence listed in Table 5.

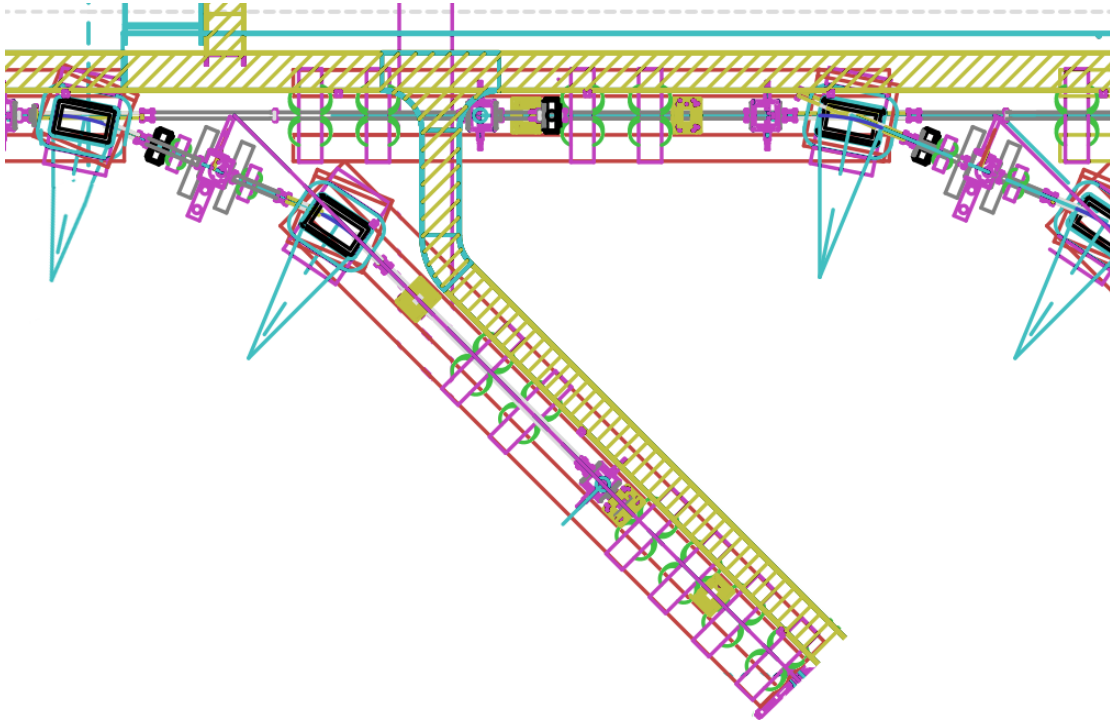


Figure 7: Design drawing `ISK0141D.dwg`, showing an overview of the second half of sequence `hebt2_db0`, spanning HEBT2:MB0 to HEBT2:Q8, visible as the central diagonal beamline segment. Note that the sequence assumes HEBT2:MB0 is on, deflecting beam into the HEBT2 line for delivery to DRAGON. The beam propagation in the present figure runs from top left to bottom right. The reference for both the beamline segment comprising both dipoles HEBT2:MB0 and MB1 is visible in Figure 4, being `IHE0120D.dwg`.

sequence hebt2_db0			
Start IHE0120D.dwg (x,y)		End IHE0120D.dwg (x,y)	
(50.382",114.593")		(159.100",110.443")	
Design Drawing		Figure 4	
Element Name	Element Type	Position S[mm]	Length L[mm]
start sequence	marker	0.000	0.000
HEBT2:MB0	mb	197.091	392.709
HEBT2:Q1	MQuad	983.640	80.000
HEBT2:Q2	MQuad	1563.649	80.000
HEBT2:MB1	mb	2349.564	392.709
Start ISK0141D.dwg (x,y)		End ISK0141D.dwg (x,y)	
(920.324",3406.143")		(1046.737",3280.338")	
Design Drawing		Figure 7	
Element Name	Element Type	Position S[mm]	Length L[mm]
HEBT2:Q3	MQuad	3864.901	180.000
HEBT2:Q4	MQuad	4394.898	180.000
HEBT2:Q5	MQuad	5684.885	180.000
HEBT2:Q6	MQuad	6164.888	180.000
HEBT2:Q7	MQuad	6644.883	180.000
HEBT2:Q8	MQuad	7124.878	180.000
end sequence	marker	7334.262	0.000

Table 5: Sequence `hebt2_db0`, showing source design drawings (.dwg files) with reference start and end coordinates from which elements and their positions along the optical axis, S in millimeters were extracted. Note: all HEBT design drawings use inches as reference units, however the `/acc` database by convention is defined in metric units. The `TRANSOPTR` element (subroutine) type, in addition to the element length are also displayed. All element positions are referenced to the drawing listed above their respective location in the table.

### 3.6 Sequence `hebt3_db0`

Beam delivery to TUDA-I is enabled by both dipole magnets HEBT3:MB0 and HEBT3:MB1, which laterally deflect beam into the HEBT3 line. As such, the sequence `hebt3_db0` is defined at the start of the curved reference trajectory through HEBT3:MB0, starting off where `hebt_db12` ends, visible in Figure 6. The sub-sequences, design drawings and start/end points defining `hebt3_db0` are listed in Table 6. Beyond HEBT3:MB1, the remaining straight segment comprising the HEBT3 line is shown in Figure 8, with the overall layout of the sequence listed in Table 6.

sequence hebt3_db0			
Start IHE0064D.dwg (x,y)		End IHE0064D.dwg (x,y)	
(33.427cm,477.193cm)		(846.746cm,551.863cm)	
Design Drawing		Figure 8	
Element Name	Element Type	Position S[mm]	Length L[mm]
start sequence	marker	0.000	0.000
HEBT3:MB0	mb	196.350	392.700
HEBT3:Q1	MQuad	982.901	80.000
HEBT3:Q2	MQuad	1562.916	80.000
HEBT3:MB1	mb	2339.320	392.700
HEBT3:Q3	MQuad	3915.710	180.000
HEBT3:Q4	MQuad	4445.710	180.000
HEBT3:Q5	MQuad	6570.640	250.000
HEBT3:Q6	MQuad	7120.620	250.000
HEBT3:Q7	MQuad	7770.620	250.000
HEBT3:Q8	MQuad	8320.620	250.000
end sequence	marker	8605.435	0.000

Table 6: Sequence hebt3\_db0, showing source design drawing (.dwg file) with reference start and end coordinates from which elements and their positions along the optical axis, S in millimeters were extracted. The TRANSOPTR element (subroutine) type, in addition to the element length are also displayed. All element positions are referenced to the drawing listed above their respective location in the table. Observe quadrupoles HEBT3:Q5 to Q8 differ from the standard HEBT quadrupole designs, featuring an effective length of 250.000mm each.

With regards to the choice of design drawing for the hebt3\_db0 sequence, one will observe that there is a drawing overlap with ISK0129D.dwg, shown previously in Figure 6 and used for the sequence hebt\_db16. The design drawing shown in Figure 8 was chosen for the present sequence as it spans the entirety of the sequence within a single drawing, removing the need to cross-reference drawings.

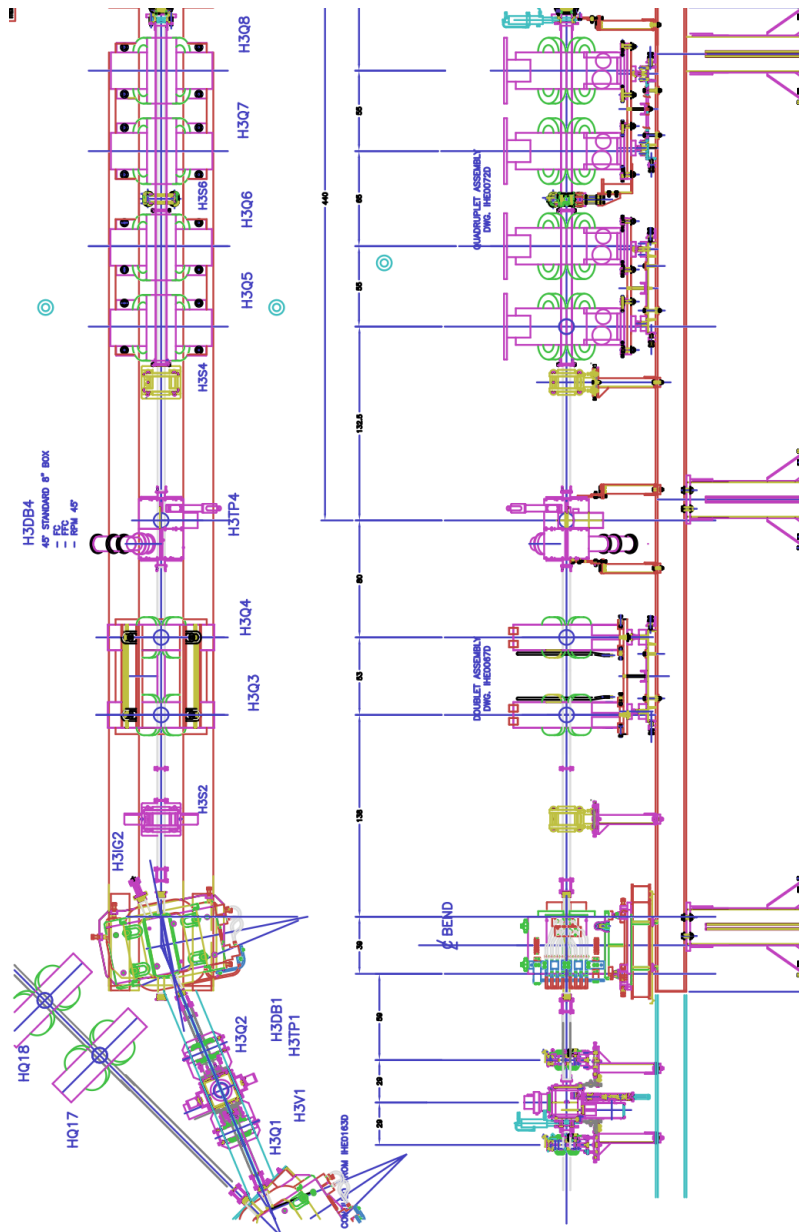


Figure 8: Design drawing IHE0064D.dwg, showing an overview of the sequence hebt3\_db0, spanning HEBT3:MB0 to HEBT3:Q8. The sequence hebt3\_db0 assumes HEBT3:MB0 is powered and deflects beam laterally into the TUDA-I line. The beam propagation in the present figure runs from bottom to top.

## 4 HEBT RF Cavities

TRANSOPTR accelerating (or bunching) simulations rely upon calls to the subroutine `linac`, which itself expects as input a handfull of cavity design parameters. These include the RF

phase setting of the cavity and the operating frequency in MHz. As is outlined in Reference [4], for the case of axially symmetric RF accelerating geometries, the F-matrix representing the cavity effects upon the moments of the beam distribution may be expressed as:

$$\mathbf{F}_{\mathbf{R}}(s) = \begin{pmatrix} 0 & \frac{1}{P_0} & 0 & 0 & 0 & 0 \\ \mathcal{A}(s) & 0 & 0 & 0 & 0 & 0 \\ 0 & 0 & 0 & \frac{1}{P_0} & 0 & 0 \\ 0 & 0 & \mathcal{A}(s) & 0 & 0 & 0 \\ 0 & 0 & 0 & 0 & \frac{\beta'}{\beta} & \frac{1}{\gamma^2 P_0} \\ 0 & 0 & 0 & 0 & \mathcal{B}(s) & -\frac{\beta'}{\beta} \end{pmatrix} \quad (1)$$

with the functions:

$$\mathcal{A}(s) = -\frac{q}{2\beta c} \left( \mathcal{E}'(s)C - \mathcal{E}(s)S \frac{\omega\beta}{c} \right) \quad (2)$$

$$\mathcal{B}(s) = \frac{q\mathcal{E}(s)\omega S}{\beta^2 c^2} \quad (3)$$

where the parameters  $S = \sin(\omega t_0 + \theta)$  and  $C = \cos(\omega t_0 + \theta)$  and  $\mathcal{E}(s)$  &  $\mathcal{E}'(s)$  is the on-axis electric field and its derivative with respect to  $s$ , the distance along the optical axis. Providing this field mapping is therefore indispensable for implementing the envelope simulation.

#### 4.1 Opera2D RF Cavity Simulations

The HEBT section contains two bunchers designed to allow for supplemental beam bunching on DTL accelerated beams slated for delivery to the ISAC-I high energy sections, which includes the DRAGON and TUDA-I experiment, in addition to the 0° experimental station at the end of the HEBT line. Both bunchers are designed for different input beam energies, listed in Table 7. The table includes references to the TRIUMF Design Office technical drawings from which the cavity parameters were extracted for the Opera2D simulation.

Buncher	$f$ [MHz]	E-range [MeV/u]	ref. DWG
HEBT-11MHz (low-beta)	11.78	0.15-0.4	IRF1483D.dwg
HEBT-35MHz (high-beta)	35.36	0.4-1.5	IRF1351D.dwg

Table 7: Both HEBT bunchers, their operating frequencies and their designed energy range [5]. The designation low and high-beta refer to the respective input energy range for both devices.

The design drawings featuring both bunchers are shown below, with the 11MHz low-beta buncher in Figure 9 and the 35MHz high-beta in Figure 10, corresponding to the drawings

listed in Table 7. In the case of the 11MHz low-beta buncher, the parameters extracted from design drawing IRF1483D.dwg are presented in Table 8, as used for the Opera2D electric field simulation. Likewise, the parameters for the 35MHz high-beta buncher are shown in Table 9.

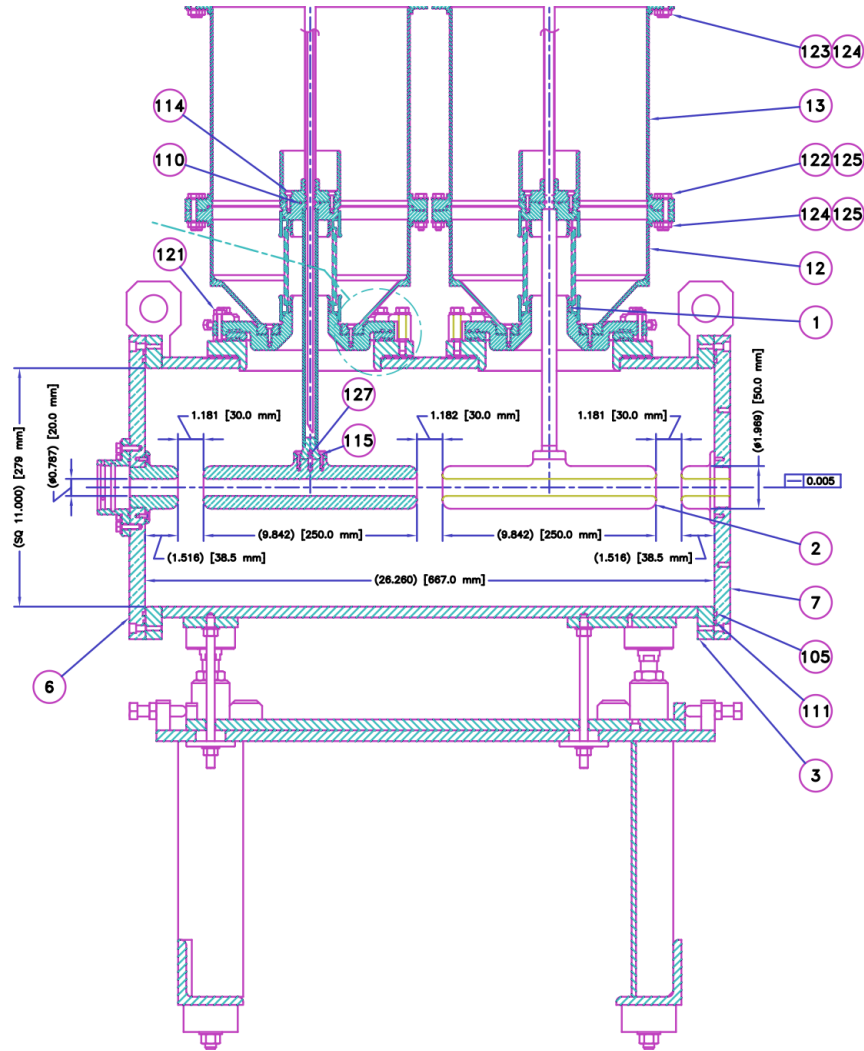


Figure 9: Design drawing IRF1483D.dwg, showing interior detail for the HEBT 11MHz low-beta buncher. Obtained from the TRIUMF Design Office.



Parameter	Value [in]
Start	0.0000
ground tube end	2.2410
tube 1 start	3.4220
tube 1 end	13.2640
tube 2 start	14.4460
tube 2 end	24.2880
ground tube start	25.4690
ground tube end	27.7100
aperture radius	0.3935
radial tube thickness	0.5910
inner-tube rounding radius	0.1875
outer tube rounding radius	0.3750
full field-map length	27.7100

Table 8: Physical dimensions extracted from drawing IRF1483D.dwg for the HEBT 11MHz low-beta buncher.

Parameter	Value [in]
Start	0.0000
ground tube end	4.2920
tube 1 start	5.7095
tube 1 end	9.6465
ground tube start	11.0640
ground tube end	15.3710
aperture radius	0.3937
radial tube thickness	0.5906
inner-tube rounding radius	0.1875
outer tube rounding radius	0.3750
full field-map length	15.3710

Table 9: Physical dimensions extracted from drawing IRF1351D.dwg for the HEBT 35MHz high-beta buncher.

The simulated on-axis longitudinal electric fields for both devices, as obtained from `Opera2D`, are shown in Figures 11 and 12, respectively. Both of these provide `TRANSDPTR` with the requisite  $\mathcal{E}(s)$ , visible in Eqs. (1), (2) and (3), required for a call to the subroutine `linac`, enabling simulations of supplemental beam bunching provided by the HEBT bunchers, for ISAC-I high energy experiment beam delivery.

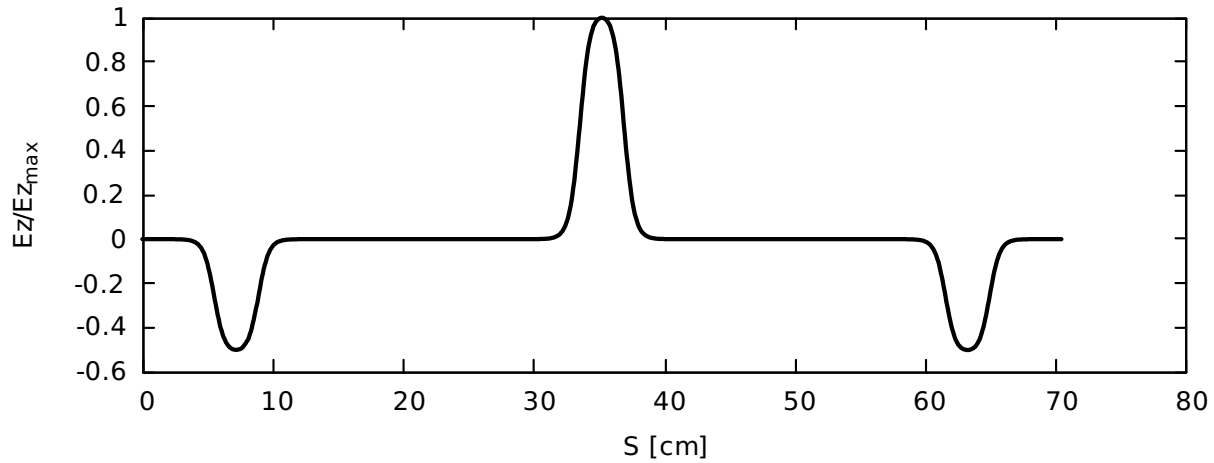


Figure 11: `Opera2D` simulated normalized on-axis electric field for the HEBT 11MHz low-beta buncher, using the parameters specified in Table 8.

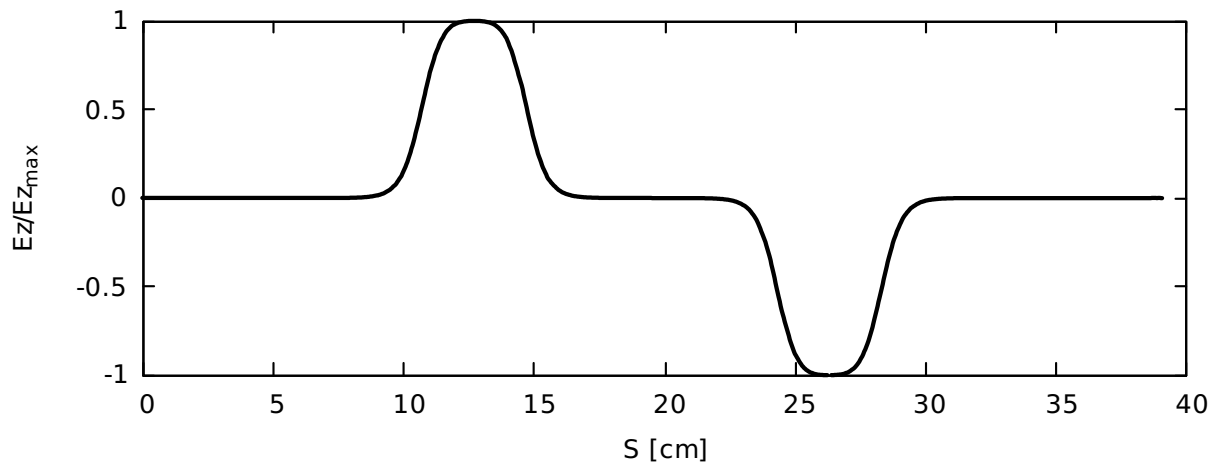


Figure 12: `Opera2D` simulated normalized on-axis electric field for the HEBT 35MHz high-beta buncher, using the parameters specified in Table 9.

## 5 Trace-3D Simulations

The Trace-3D implementation for the HEBT beamlines are segmented into groups of roughly 5 quadrupoles each, as specified in Table 10. Additionally, the table features beam parameters used for the original simulations. The ensemble of simulations shown in Table 10 and the listed figures represent the tune computation and analysis tools which were used for the ISAC-I high energy sections up until 2019.

Figure ref.	subsequence elements	$m[\text{MeV}/c^2]$	E [MeV]	Q
Figure 13	HEBT:Q1 to HEBT:Q5	27944.83	45.00	5
Figure 14	HEBT:Q6 to HEBT:Q10	27944.83	45.00	5
Figure 15	HEBT:Q11 to HEBT:Q18	21580.44	34.50	5
Figure 16	HEBT:Q6 to Prague	27944.83	45.00	5
Figure 17	HEBT:Q11 to HEBT2:Q4	27944.83	45.00	5
Figure 18	HEBT2:Q5 to DRAGON	27944.83	45.00	5
Figure 19	HEBT:Q15 to HEBT3:Q4	27944.83	45.00	5
Figure 20	HEBT3:Q5 to TUDA-I	27944.83	45.00	5

Table 10: Listing of Trace-3D HEBT simulations, as used by the TRIUMF Beam Physics group to compute ISAC-I high energy tunes, with associated figures showing original simulation outputs. Input particle mass, energy and charge state are also listed, as they were on the original .t3d files.

It is worth noting that, for all simulations listed above, no assumptions are made with regard to longitudinal beam bunching. Inspection of Figures 13 to 20 reveals that from the longitudinal beam dynamics standpoint, the former is either treated as a continuous beam or does not have specified starting parameters for coordinates  $(z, P_z)$ , for example in Figure 16.

As the purpose of the present note is to establish the validity of the TRANSOPTR implementation via the /acc database compared to Trace-3D, the performance of the HEBT buncher implementation will be reserved for a later note. At present, it will simply be noted that the bunchers have been implemented in TRANSOPTR, following the same outlined methodology in [2], and using the fields  $\mathcal{E}(s)$  shown in Figures 11 and 12.

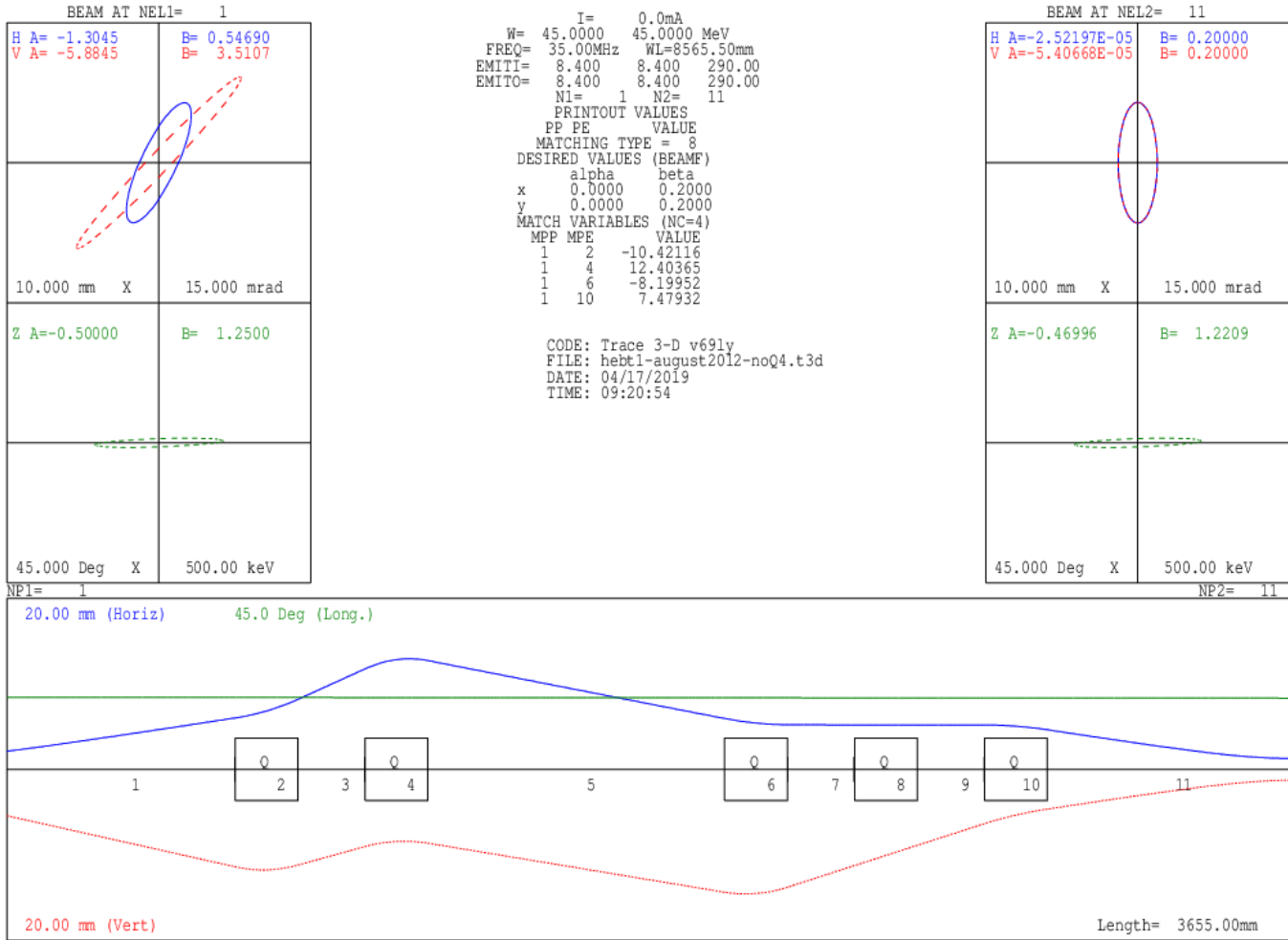


Figure 13: Trace-3D envelope simulation of sub-sequence spanning HEBT:Q1 to HEBT:Q5. The horizontal envelope and its parameters are shown in blue, vertical in red and longitudinal in green. The input beam ellipses containing  $4\epsilon_{RMS}$  are shown on the left hand side, with A and B representing the Twiss parameters  $\alpha$  and  $\beta$ , while the output distributions are on the right hand side. The input and output beam emittances are visible in the top center, labeled EMITI and EMITO, respectively, and have units of mm\*mrad for transverse and deg\*keV for longitudinal. The beam envelopes are shown at the bottom, following the same color convention. The location and lengths of quadrupoles are represented by the squares labeled Q. Drifts are represented by a black horizontal line at the lower graph midplane. Finally, the numbers on the lower graph, spanning 1 to 11, sequentially label all elements called in the simulation. Quadrupole gradients are shown in Table 11.

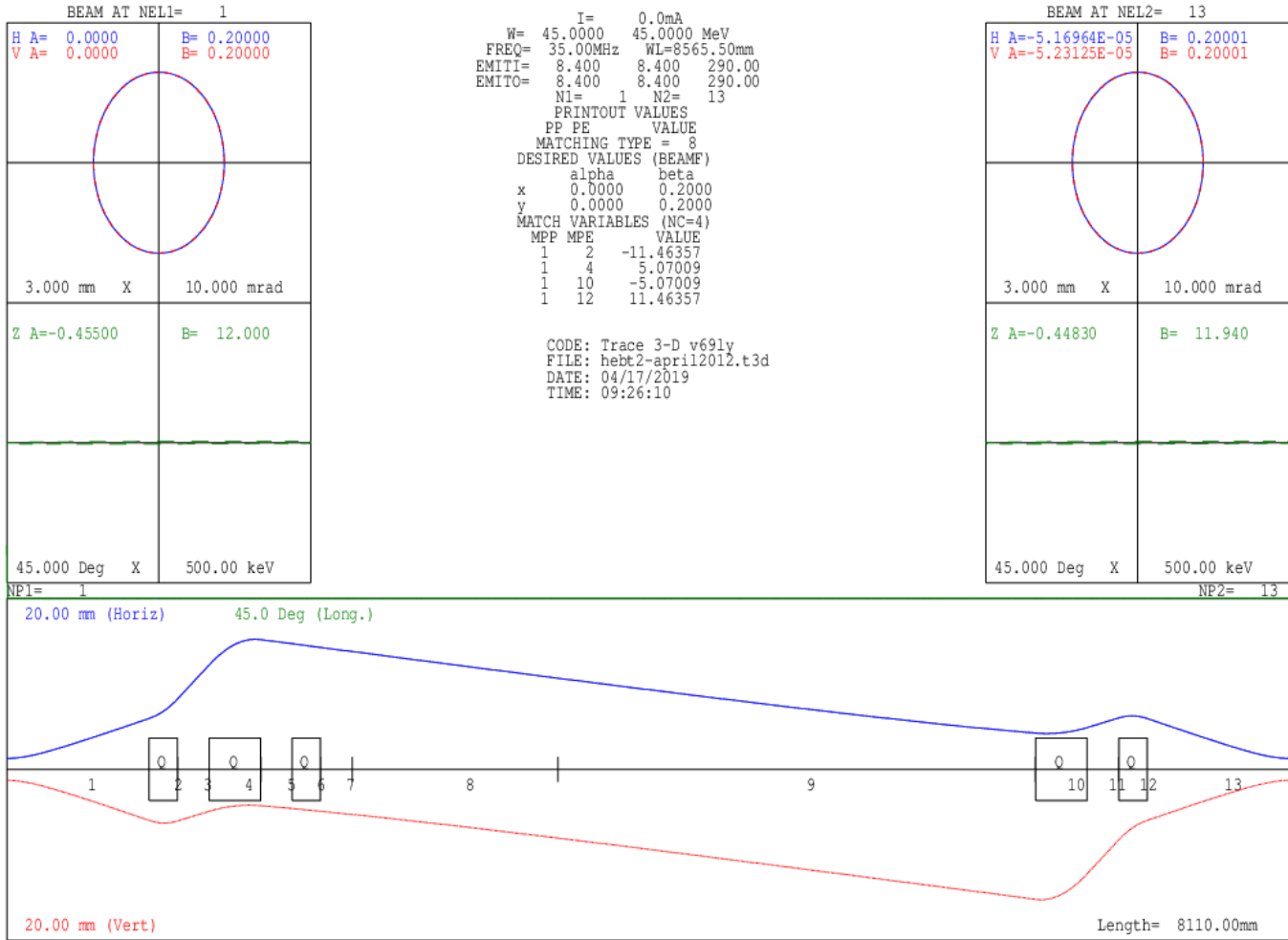


Figure 14: Trace-3D envelope simulation of sub-sequence spanning HEBT:Q6 to HEBT:Q10. The horizontal envelope and its parameters are shown in blue, vertical in red and longitudinal in green. The input beam ellipses containing  $4\epsilon_{RMS}$  are shown on the left hand side, with A and B representing the Twiss parameters  $\alpha$  and  $\beta$ , while the output distributions are on the right hand side. The input and output beam emittances are visible in the top center, labeled EMITI and EMITO, respectively, and have units of mm\*mrad for transverse and deg\*keV for longitudinal. The beam envelopes are shown at the bottom, following the same color convention. The location and lengths of quadrupoles are represented by the squares labeled Q. Drifts are represented by a black horizontal line at the lower graph midplane. Finally, the numbers on the lower graph, spanning 1 to 13, sequentially label all elements called in the simulation. Quadrupole gradients are shown in Table 11.

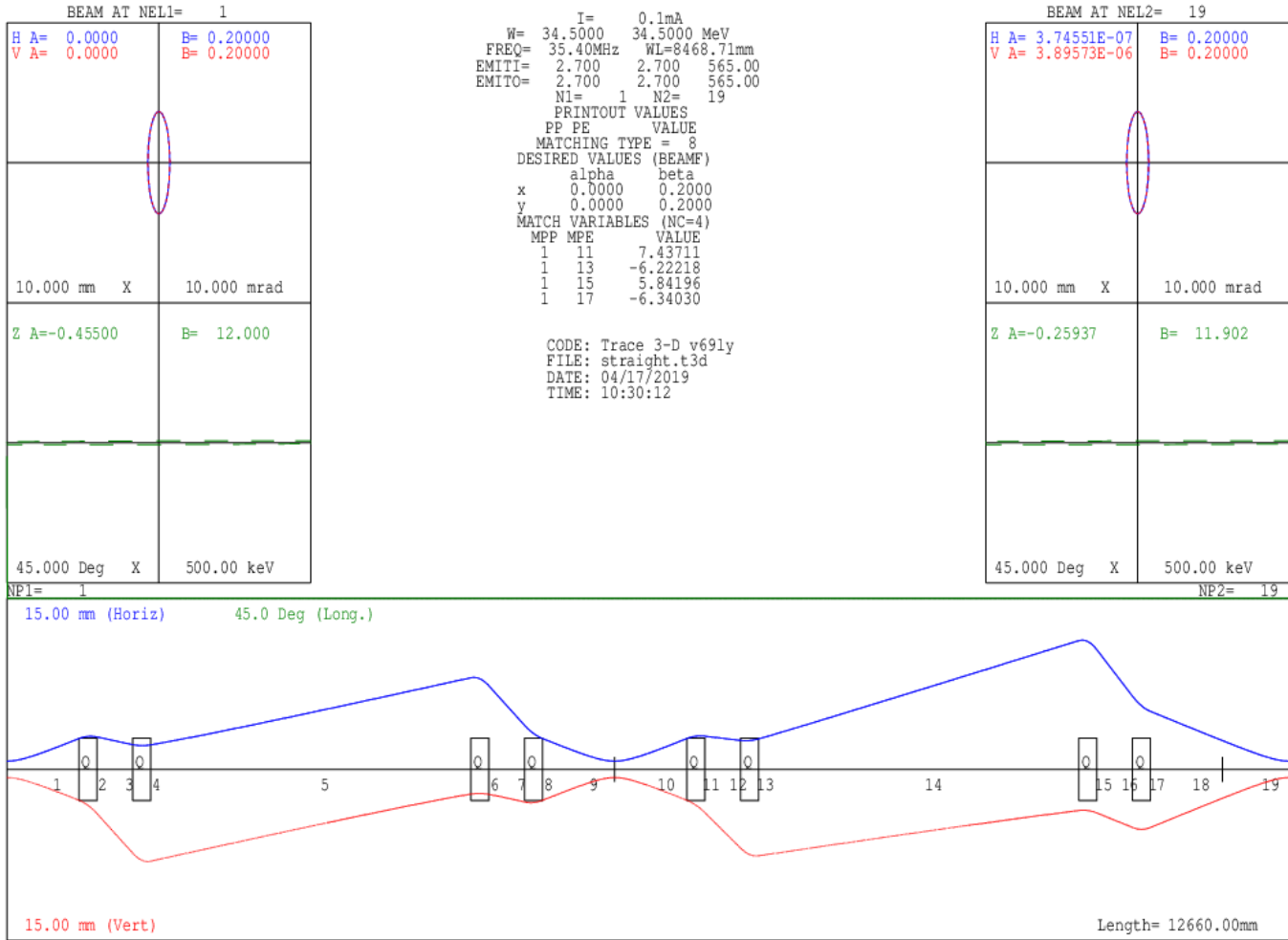


Figure 15: Trace-3D envelope simulation of sub-sequences spanning HEBT:Q11 to HEBT:Q18, followed by a drift representing injection in the HEBT 0° experiment station. The horizontal envelope and its parameters are shown in blue, vertical in red and longitudinal in green. The input beam ellipses containing  $4\epsilon_{RMS}$  are shown on the left hand side, with A and B representing the Twiss parameters  $\alpha$  and  $\beta$ , while the output distributions are on the right hand side. The input and output beam emittances are visible in the top center, labeled EMITI and EMITO, respectively, and have units of mm\*mrad for transverse and deg\*keV for longitudinal. The beam envelopes are shown at the bottom, following the same color convention. The location and lengths of quadrupoles are represented by the squares labeled Q. Drifts are represented by a black horizontal line at the lower graph midplane. Finally, the numbers on the lower graph, spanning 1 to 19, sequentially label all elements called in the simulation. Quadrupole gradients are shown in Table 13.

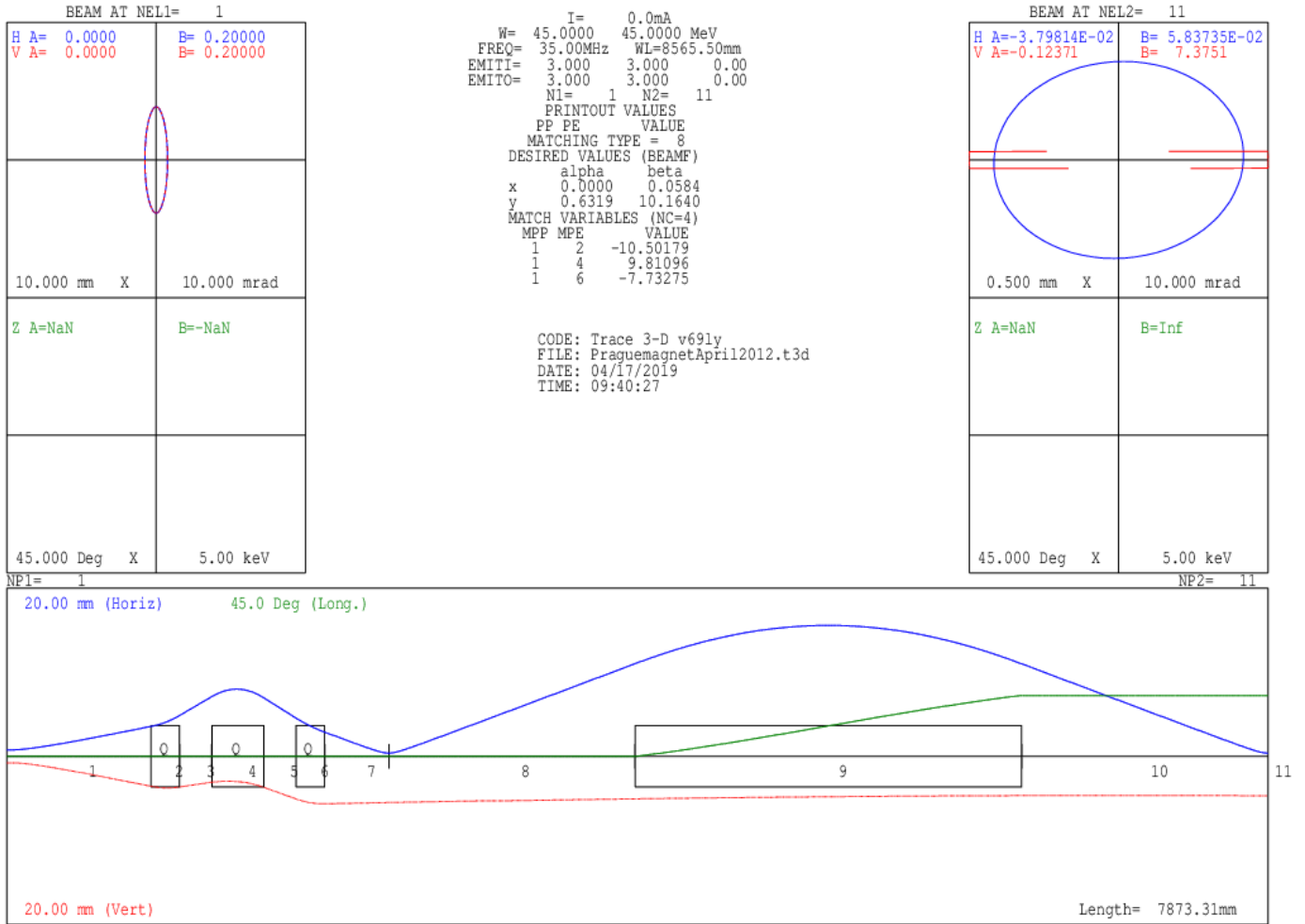


Figure 16: Trace-3D envelope simulation of sub-sequence spanning HEBT:Q6 to the diagnostic station after the Prague magnet (HEBT1:MB0). The horizontal envelope and its parameters are shown in blue, vertical in red and longitudinal in green. The input beam ellipses containing  $4\epsilon_{RMS}$  are shown on the left hand side, with A and B representing the Twiss parameters  $\alpha$  and  $\beta$ , while the output distributions are on the right hand side. The input and output beam emittances are visible in the top center, labeled EMITI and EMITO, respectively, and have units of mm\*mrad for transverse and deg\*keV for longitudinal. The beam envelopes are shown at the bottom, following the same color convention. The location and lengths of quadrupoles are represented by the squares labeled Q. Drifts are represented by a black horizontal line at the lower graph midplane. Finally, the numbers on the lower graph, spanning 1 to 11, sequentially label all elements called in the simulation. Quadrupole gradients are shown in Table 12.

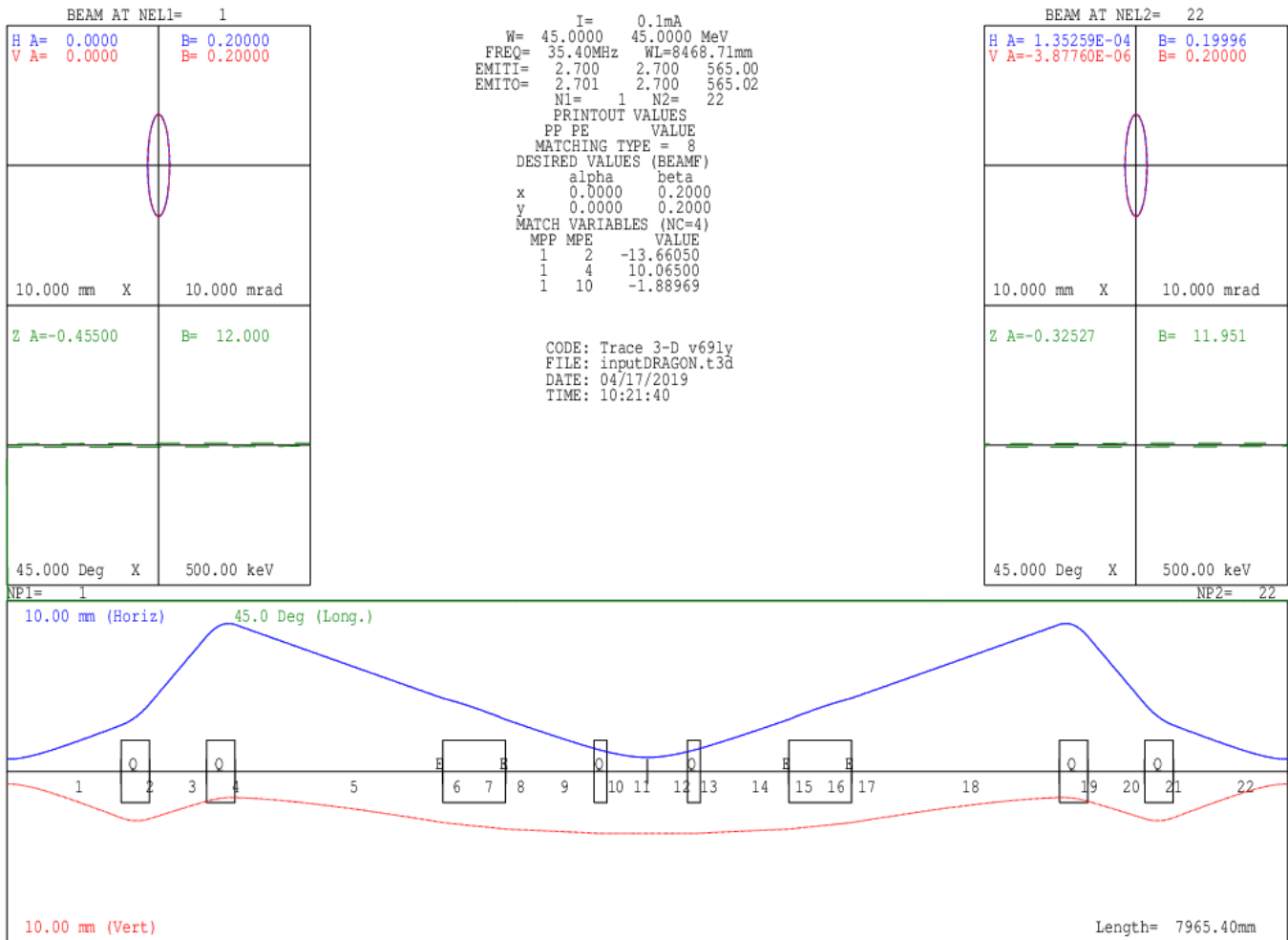


Figure 17: Trace-3D envelope simulation of sub-sequence spanning HEBT:Q11 to HEBT2:Q4 after lateral beam deflection into the HEBT2 line via HEBT2:MB0 and MB1. The horizontal envelope and its parameters are shown in blue, vertical in red and longitudinal in green. The input beam ellipses containing  $4\epsilon_{RMS}$  are shown on the left hand side, with A and B representing the Twiss parameters  $\alpha$  and  $\beta$ , while the output distributions are on the right hand side. The input and output beam emittances are visible in the top center, labeled EMITI and EMITO, respectively, and have units of mm\*mrad for transverse and deg\*keV for longitudinal. The beam envelopes are shown at the bottom, following the same color convention. The location and lengths of quadrupoles are represented by the squares labeled Q. Drifts are represented by a black horizontal line at the lower graph midplane. Finally, the numbers on the lower graph, spanning 1 to 22, sequentially label all elements called in the simulation. Quadrupole gradients are shown in Table 13.

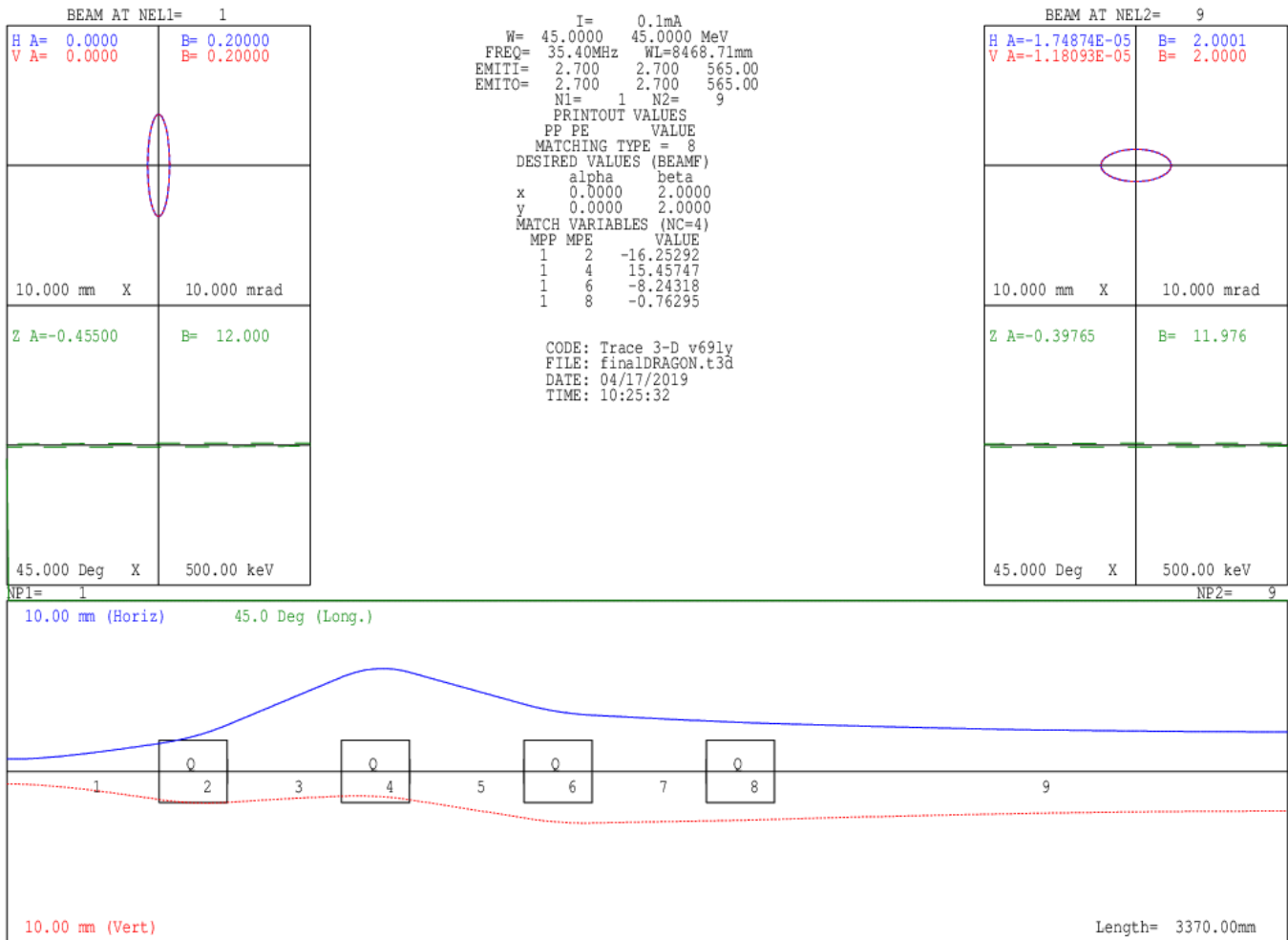


Figure 18: Trace-3D envelope simulation of sub-sequence spanning HEBT2:Q5 to HEBT2:Q8 including a straight drift section representing injection in the DRAGON experiment. The horizontal envelope and its parameters are shown in blue, vertical in red and longitudinal in green. The input beam ellipses containing  $4\epsilon_{RMS}$  are shown on the left hand side, with A and B representing the Twiss parameters  $\alpha$  and  $\beta$ , while the output distributions are on the right hand side. The input and output beam emittances are visible in the top center, labeled EMITI and EMITO, respectively, and have units of mm\*mrad for transverse and deg\*keV for longitudinal. The beam envelopes are shown at the bottom, following the same color convention. The location and lengths of quadrupoles are represented by the squares labeled Q. Drifts are represented by a black horizontal line at the lower graph midplane. Finally, the numbers on the lower graph, spanning 1 to 9, sequentially label all elements called in the simulation. Quadrupole gradients are shown in Table 14.

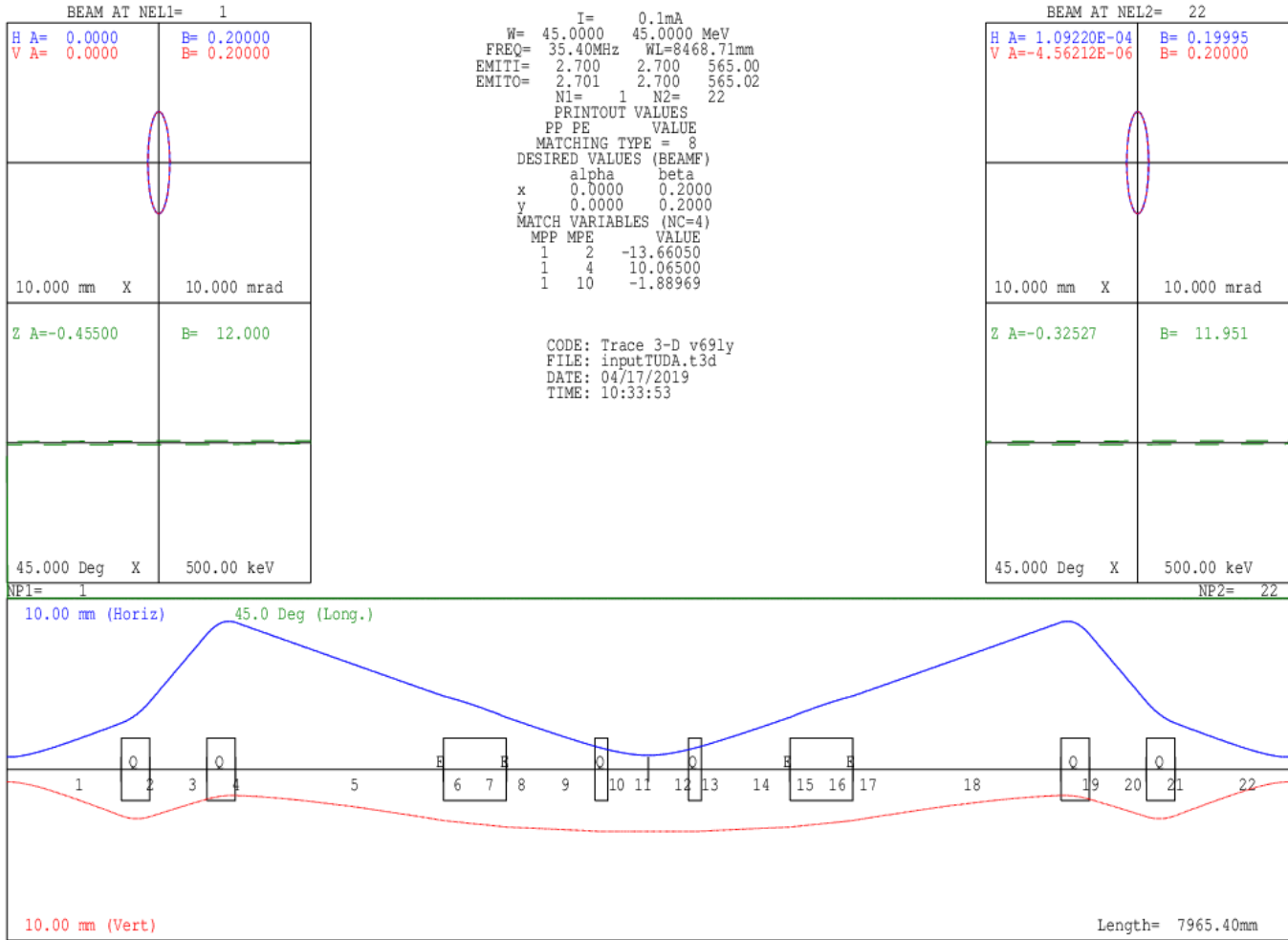


Figure 19: Trace-3D envelope simulation of sub-sequence spanning HEBT:Q15 to HEBT3:Q4 after lateral beam deflection into the HEBT3 line via HEBT3:MB0 and MB1. The horizontal envelope and its parameters are shown in blue, vertical in red and longitudinal in green. The input beam ellipses containing  $4\epsilon_{RMS}$  are shown on the left hand side, with A and B representing the Twiss parameters  $\alpha$  and  $\beta$ , while the output distributions are on the right hand side. The input and output beam emittances are visible in the top center, labeled EMITI and EMITO, respectively, and have units of mm\*mrad for transverse and deg\*keV for longitudinal. The beam envelopes are shown at the bottom, following the same color convention. The location and lengths of quadrupoles are represented by the squares labeled Q. Drifts are represented by a black horizontal line at the lower graph midplane. Finally, the numbers on the lower graph, spanning 1 to 22, sequentially label all elements called in the simulation. Quadrupole gradients are shown in Table 14.



## 5.1 Trace-3D Element Setpoints

For all the Trace-3D simulations listed in Table 10, the corresponding quadrupole current settings are listed in Tables 11 to 15, shown below. Further information on ISAC HE magnetic quadrupole parameters may be found in [6].

Figure 13			Figure 14		
Magnet	Aperture [cm]	Gradient [T/m]	Magnet	Aperture [cm]	Gradient [T/m]
HEBT:Q1	2.6	-10.4212	HEBT:Q6	2.6	-11.4636
HEBT:Q2	2.6	12.4037	HEBT:Q7	2.6	5.0700
HEBT:Q3	2.6	-8.1995	HEBT:Q8	2.6	0.0000
HEBT:Q4	2.6	-	HEBT:Q9	2.6	-5.0701
HEBT:Q5	2.6	7.4793	HEBT:Q10	2.6	11.4636

Table 11: Listing of Quadrupole gradient settings for Trace-3D HEBT simulations corresponding to the specified figure, with parameters as specified in Table 10.

Figure 16		
Magnet	Aperture [cm]	Gradient [T/m]
HEBT:Q6	2.6	-10.5018
HEBT:Q7	2.6	9.8110
HEBT:Q8	2.6	-7.7328

Table 12: Listing of Quadrupole gradient settings for Trace-3D HEBT simulations corresponding to the specified figures, with parameters as specified in Table 10.

Figure 15			Figure 17		
Magnet	Aperture [cm]	Gradient [T/m]	Magnet	Aperture [cm]	Gradient [T/m]
HEBT:Q11	2.6	8.7904	HEBT:Q11	2.6	-13.6605
HEBT:Q12	2.6	-6.7867	HEBT:Q12	2.6	10.0650
HEBT:Q13	2.6	6.7867	HEBT2:Q1	1.0	-1.8897
HEBT:Q14	2.6	-8.7904	HEBT2:Q2	1.0	-1.8897
HEBT:Q15	2.6	7.4371	HEBT2:Q3	2.6	10.0650
HEBT:Q16	2.6	-6.2222	HEBT2:Q4	2.6	-13.6605
HEBT:Q17	2.6	5.8419			
HEBT:Q18	2.6	-6.3403			

Table 13: Listing of Quadrupole gradient settings for Trace-3D HEBT simulations corresponding to the specified figures, with parameters as specified in Table 10.

Figure 18			Figure 19		
Magnet	Aperture [cm]	Gradient [T/m]	Magnet	Aperture [cm]	Gradient [T/m]
HEBT2:Q5	2.6	-16.2529	HEBT:Q15	2.6	-13.6605
HEBT2:Q6	2.6	15.4575	HEBT:Q16	2.6	10.0650
HEBT2:Q7	2.6	-8.2432	HEBT3:Q1	1.0	-1.8897
HEBT2:Q8	2.6	-0.7630	HEBT3:Q2	1.0	-1.8897
			HEBT3:Q3	2.6	10.0650
			HEBT3:Q4	2.6	-13.6605

Table 14: Listing of quadrupole gradient settings for Trace-3D HEBT simulations corresponding to the specified figures, with parameters as specified in Table 10.

Figure 20		
Magnet	Aperture [cm]	Gradient [T/m]
HEBT3:Q5	4.2494	-4.0893
HEBT3:Q6	4.2494	7.8926
HEBT3:Q7	4.2494	-7.8926
HEBT3:Q8	4.2494	4.0893

Table 15: Listing of quadrupole gradient settings for Trace-3D HEBT simulations corresponding to the specified figure, with parameters as specified in Table 10.

## 6 TRANSOPTR Implementation of the HEBT Beamlines

The sequences discussed in Section 5 are summarized in Table 16 for clarity. As part of benchmarking, these were used to generate TRANSOPTR `sy.f` call stacks which mimic the original Trace-3D files which are mentioned in Table 10, in order to produce a comparison between both envelopes. It is reiterated that this the present comparison is not intended as a commentary on the validity or performance of both models. Instead, the comparison is chiefly produced to ensure the database is properly defined, in addition to verifying the validity of the optical parameters supplied for each beamline-optical element.

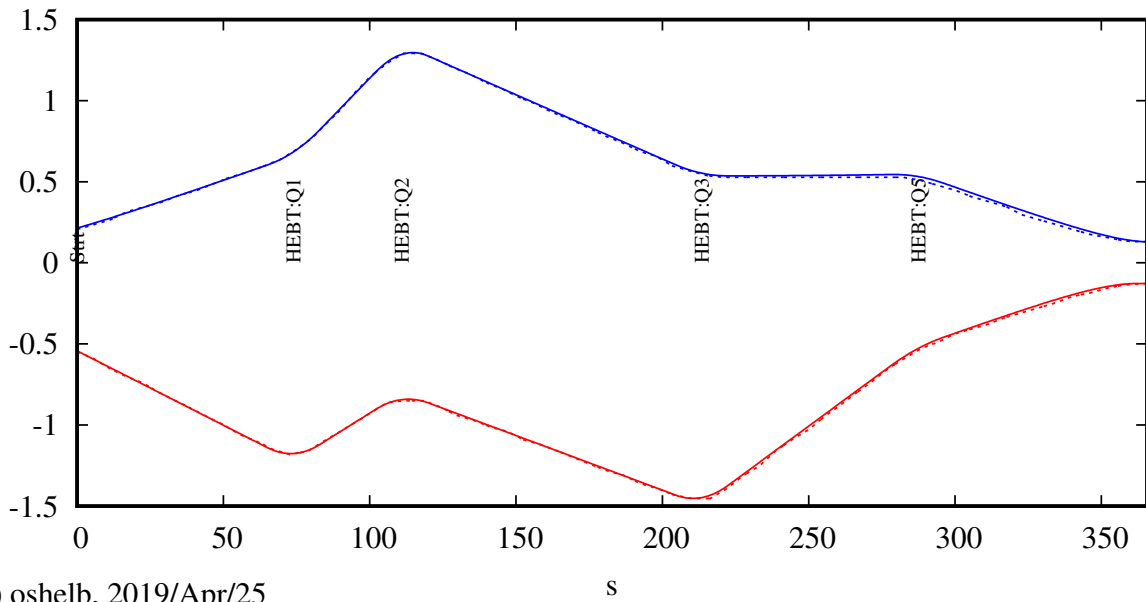
sequence	elements spanned
hebt_db0	DTL output to HEBT:Q8
hebt_db9	HEBT:Q9 to HEBT:Q12
hebt_db12	HEBT2:MB0 (off) to HEBT:Q16
hebt_db16	HEBT:Q17 to HEBT 0° Station
hebt2_db0	HEBT2:MB0 to DRAGON
hebt3_db0	HEBT3:MB0 to TUDA-I

Table 16: Listing of `/acc` database HEBT sequences including a qualitative description of the rough beampath represented by each. Note that the three ISAC-I high energy experimental sections referenced (DRAGON, TUDA-I and HEBT 0°) are at present excluded from the `/acc` database. As such, the sequences end at the experiment boundary. In the case of DRAGON and TUDA-I, these are HEBT2:IV8 and HEBT3:IV8, respectively, while for HEBT 0° it is HEBT:IV18. Descriptions for experiment sequences will be added at a later time.

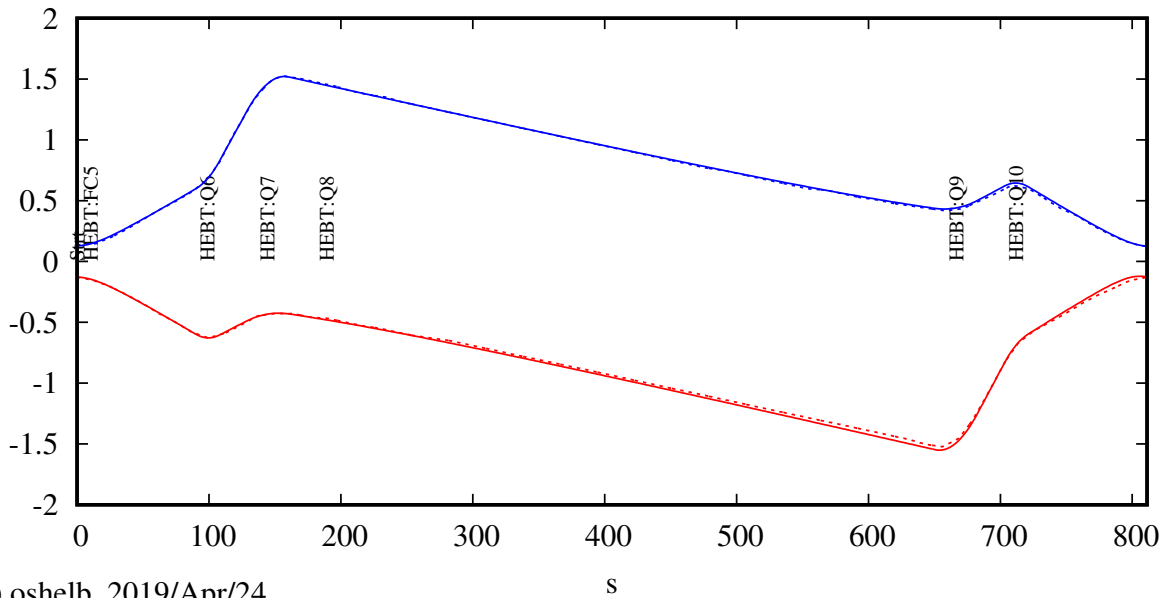
As a test of proper implementation, the sequences of Table 16 were used to generate beamline segments in TRANSOPTR matching the original Trace-3D segments, previously listed in Table 10 (Figures 13 to 20). Using the python script `xml2optr`<sup>1</sup>, overlapping optr beamline segments were produced and overlayed to the corresponding Trace-3D computations. The optr simulations were given identical initial conditions and element setpoints as the trace files for comparison. Since the available Trace-3D files for benchmarking do not feature any use of the HEBT bunchers, both bunchers were omitted from the present optr comparison, though they are available if needed, with the field maps in Figures 11 and 12.

Compared envelopes are shown below, spanning Figures 21 to 24, reproducing all listed Trace-3D segments from Table 10. For all displayed plots, all dimensions are in cm, TRANSOPTR envelopes are solid lines and Trace-3D are dotted, with identical colors representing identical envelopes (x:blue, y:red). Broad agreement is achieved between implementations.

<sup>1</sup>credit: Paul Jung & Thomas Planche

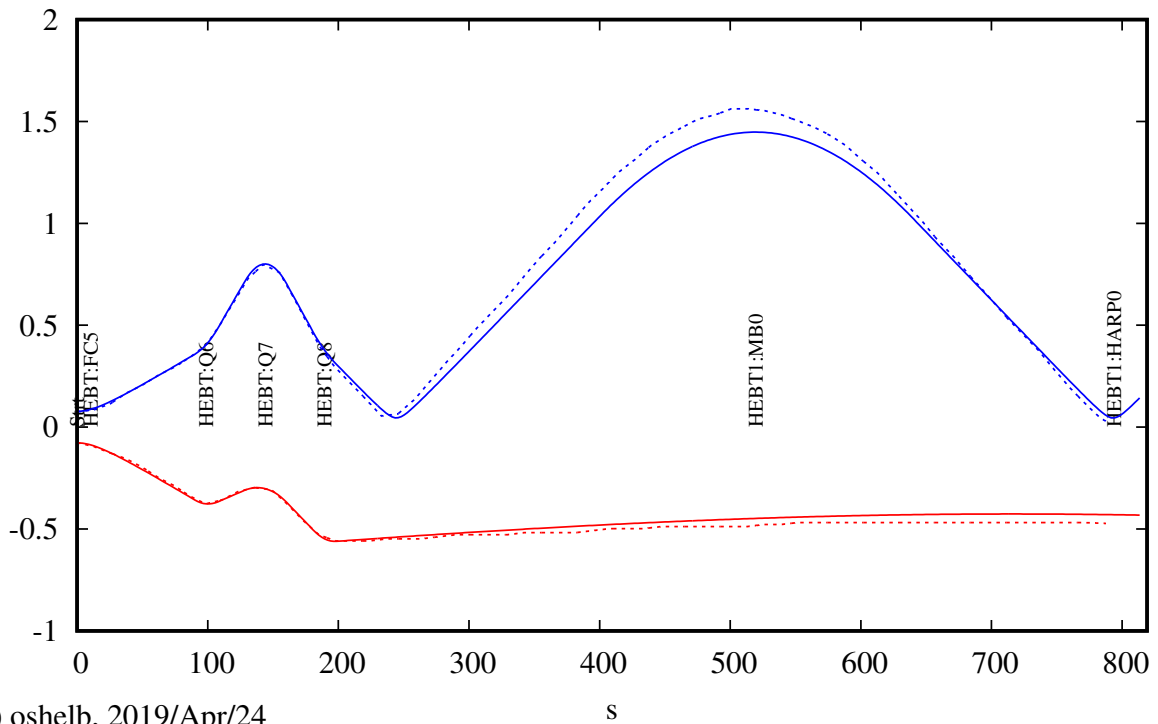


(c) oshelb, 2019/Apr/25

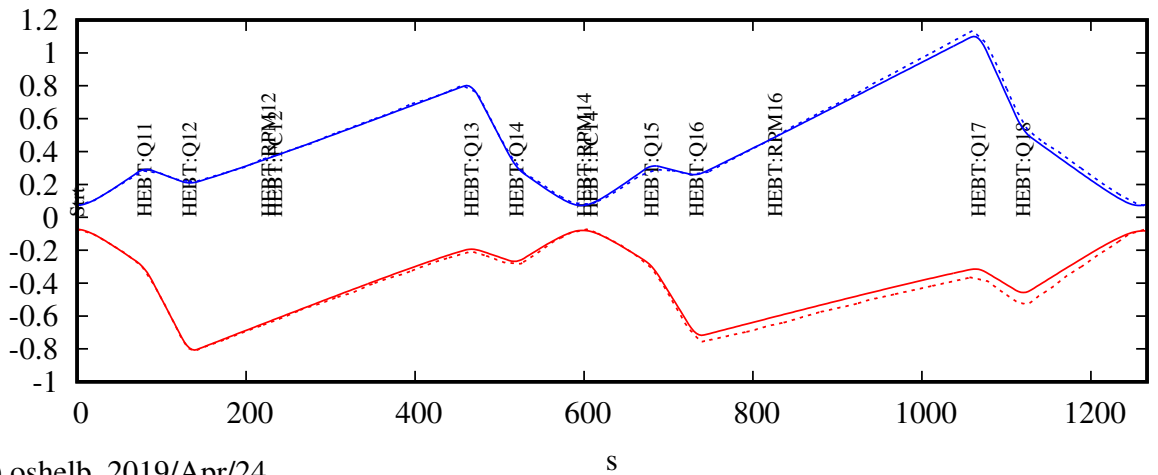


(c) oshelb, 2019/Apr/24

Figure 21: TRANSOPTR envelope simulation (solid lines), overlaid with the Trace-3D envelope (dashed lines), for the sub-sequences spanning HEBT:Q1 to Q5 (top), HEBT:Q6 to Q10 (bottom). The horizontal envelopes are shown in blue and vertical in red. Element names, as represented in the TRANSOPTR HEBT sequences are shown vertically at the graph midplanes. All x and y-axis dimensions are in cm.

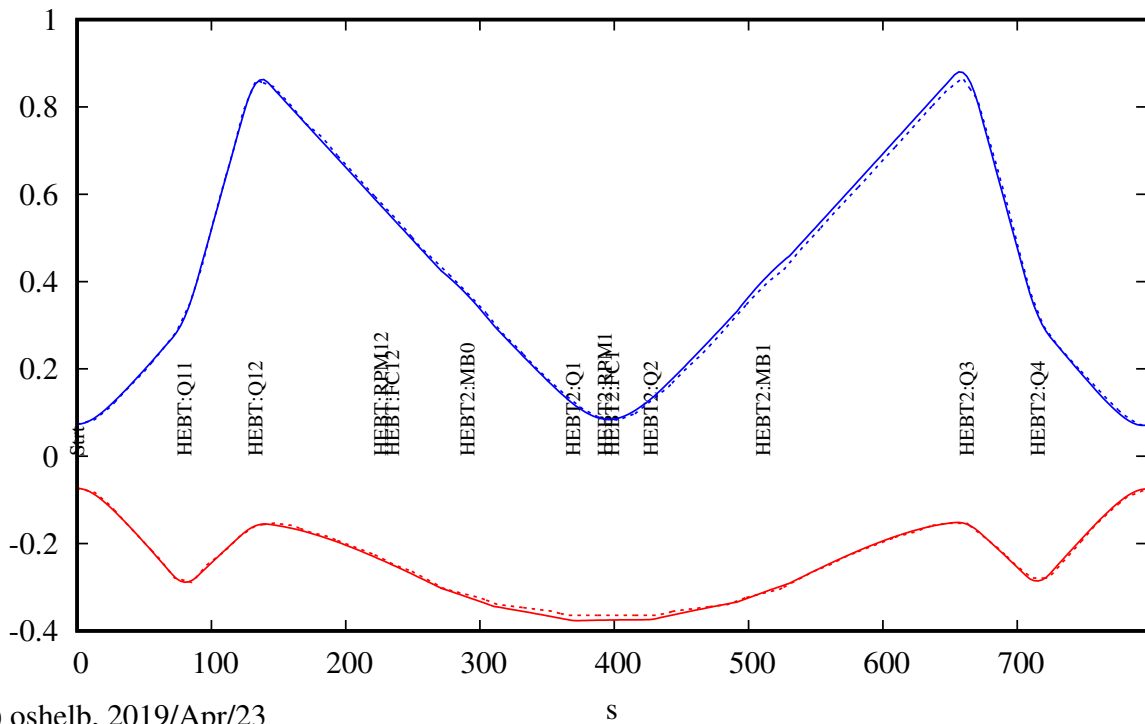


(c) oshelb, 2019/Apr/24

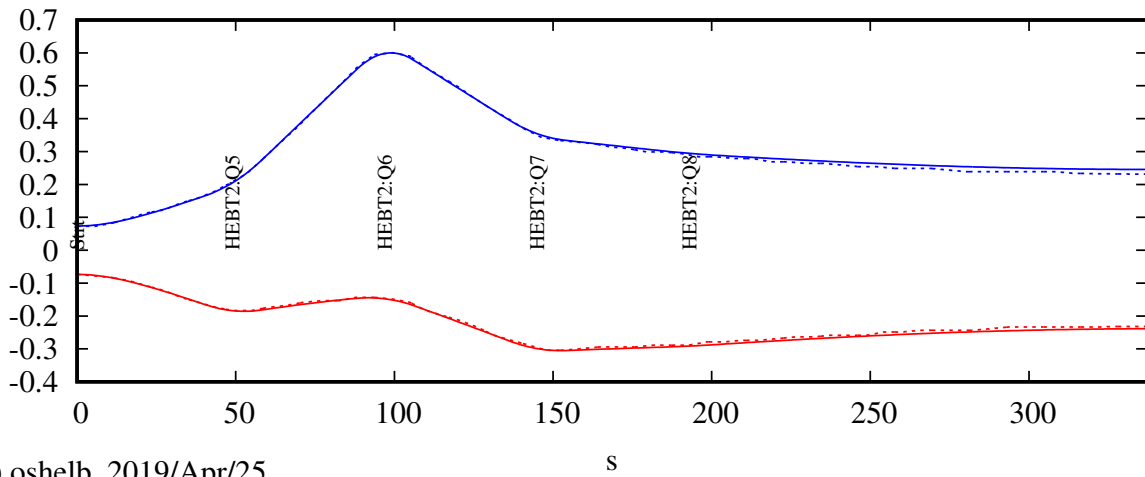


(c) oshelb, 2019/Apr/24

Figure 22: TRANSOPTR envelope simulation (solid lines), overlaid with the Trace-3D envelope (dashed lines), for the sub-sequences spanning HEBT:Q6 to Prague analyzing magnet (top) and HEBT:Q11 to Q18 (bottom), for injection in the HEBT 0° station. The horizontal envelopes are shown in blue and vertical in red. Element names, as represented in the TRANSOPTR HEBT sequences are shown vertically at the graph midplanes. All x and y-axis dimensions are in cm.

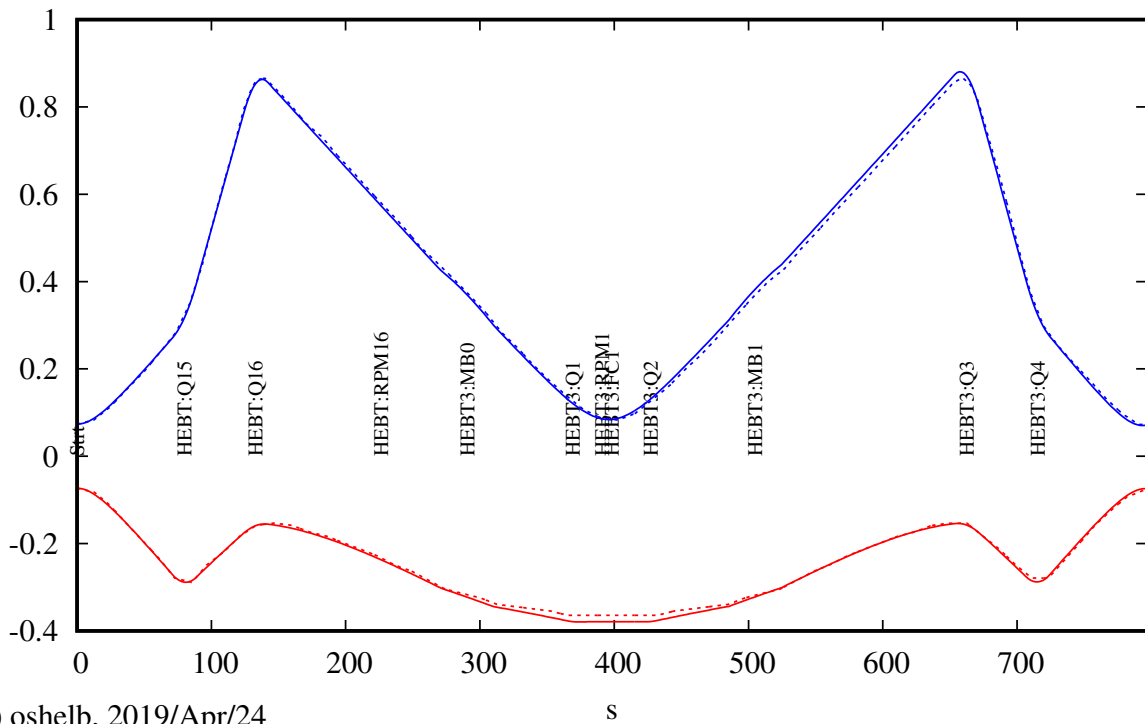


(c) oshelb, 2019/Apr/23

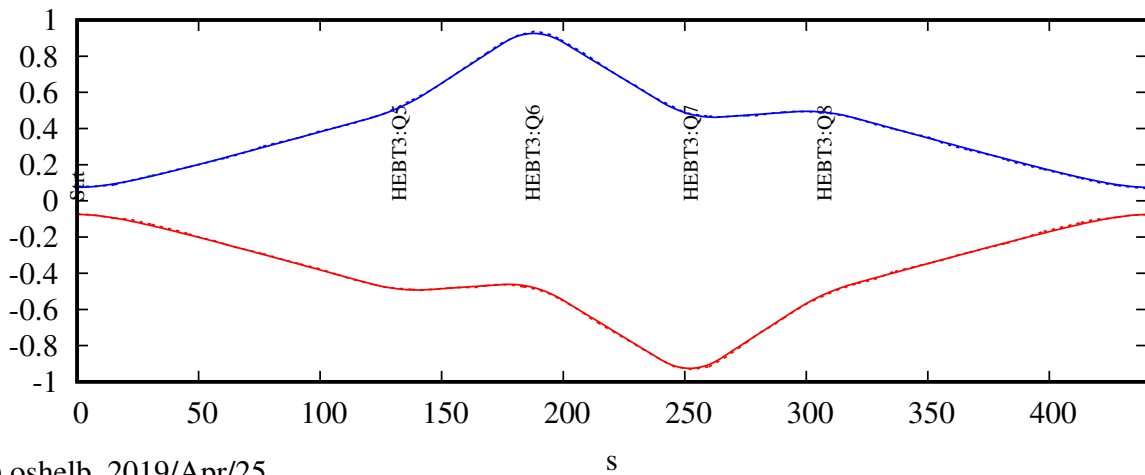


(c) oshelb, 2019/Apr/25

Figure 23: TRANSOPTR envelope simulation (solid lines), overlaid with the Trace-3D envelope (dashed lines), for the sub-sequences spanning HEFT:Q11 to HEFT2:Q4 (top) and HEFT2:Q5 to Q8 (bottom), for injection in the DRAGON experiment. The horizontal envelopes are shown in blue and vertical in red. Element names, as represented in the TRANSOPTR HEFT sequences are shown vertically at the graph midplanes. All x and y-axis dimensions are in cm.



(c) oshelb, 2019/Apr/24



(c) oshelb, 2019/Apr/25

Figure 24: TRANSOPTR envelope simulation (solid lines), overlaid with the Trace-3D envelope (dashed lines), for the sub-sequences spanning HEBT:Q15 to HEBT3:Q4 (top) and HEBT3:Q5 to Q8 (bottom), for injection in the TUDA-I experiment. The horizontal envelopes are shown in blue and vertical in red. Element names, as represented in the TRANSOPTR HEBT sequences are shown vertically at the graph midplanes. All x and y-axis dimensions are in cm.

## 7 Conclusion

In this note, the extension of `TRANSOPTR` to the ISAC-I HEBT beamlines via the TRIUMF High-Level Applications framework was demonstrated to be consistent with `Trace-3D` simulations. The former code was, up until 2019, used as the standard tool for envelope analysis and tune computation for ISAC-I High Energy tunes. While the comparisons herein produce a baseline confidence level in proper implementation of the HEBT sequences, it is stressed that these only verify what is considered by the author to be broad agreement with the underlying beam dynamics at play in the ISAC-I high energy transport.

Viewed within the overarching optic of end-to-end model development for the ISAC facility, the present work nevertheless represents a key benchmark toward the goal of providing TRIUMF with an integrated simulation, within a consistent framework, of the entire ISAC facility. It is stressed that further development work remains necessary, in particular aiming to compare actual beam-based measurements with the simulations generated by the ISAC end-to-end model.

Also, it is re-iterated that beamlines corresponding to the experimental stations for ISAC-I high-energy remain to be implemented. As a testament to the versatility of the HLA framework, these can simply be added as sequences, placed at the appropriate location with respect to the existing HEBT framework.

A further refinement will consist of the development of custom subroutines defining the HEBT quadrupoles in `TRANSOPTR`, which will feature both the as-measured effective length of the devices, in addition to an accurate implementation of the quadrupole fringe fields. At present, the `MQuad` subroutine call effectively defines a fringe-less quadrupole for the beamlines. While this agrees well with the `Trace-3D` implementation, the former implementation was made without feature fringe fields.

Finally, seeing as both HEBT bunchers were not simulated in `Trace-3D`, there remains a need to perform beam-based measurements to verify buncher behavior and compare it with the `Opera-2D` computed field maps used by `TRANSOPTR`. This issue is reserved for a later work however, as its scope will not be unique to the HEBT section. In effect, a crucial test to be performed in coming weeks shall be the undertaking of systematic verifications of `TRANSOPTR`-implemented ISAC RF cavities with beam.

## References

- [1] Laxdal RE. *Design Specification for ISAC HEBT*. Technical Report TRI-DN-99-23, TRIUMF, 1999.
- [2] Shelbaya O. *TRANSOPTR Implementation of the MEBT Beamline*. Technical Report TRI-BN-19-02, TRIUMF, 2019.
- [3] Barquest C. *Web-Based Control Room Applications at TRIUMF*. In *Proceedings of the 9th International Particle Accelerator Conference*, pages 4832–35, 2018.
- [4] Baartman R. *Fast Envelope Tracking for Space Charge Dominated Injectors*. In *Proceedings of LINAC 2016 Conference*, pages 1017–21, 2016.
- [5] AK Mitra, PJ Bricault, IV Bylinskii, K Fong, G Dutto, RE Laxdal, RL Poirier, et al. *RF Test and Commissioning of the Radio Frequency Structures of the TRIUMF ISAC I facility*. In *Proceedings of LINAC*, page 106, 2002.
- [6] R. Baartman. *B-I Curve fits for TRIUMF Quads*. Technical Report TRI-DN-07-04, TRIUMF, 2007.